RM E8L30

UNCLASSIFIED
RESTRICTED

COPY NO. 115
RM No. E8L30

NACA RM No. E8L30

NACA

RESEARCH MEMORANDUM

EXPERIMENTAL STUDY OF LOOP-SCAVENGED COMPRESSION-IGNITION CYLINDER FOR GAS-GENERATOR USE

By Hampton H. Foster, F. Ralph Schuricht
and Max J. Tauschek

Lewis Flight Propulsion Laboratory
Cleveland, Ohio

TECHNICAL LIBRARY
AIRESEARCH MANUFACTURING CO.
9851-9951 SEPULVEDA BLVD.
INGLEWOOD,
CALIFORNIA

CLASSIFIED DOCUMENT

This document contains classified information affecting the National Defense of the United States within the meaning of the Espionage Act, USC 50:31 and 32. Its transmission or the revelation of its contents in any manner to an unauthorized person is prohibited by law. Information so classified may be imparted only to persons in the military and naval services of the United States, appropriate civilian officers and employees of the Federal Government who have a legitimate interest therein, and to United States citizens of known loyalty and discretion who of necessity must be informed thereof.

NATIONAL ADVISORY COMMITTEE
FOR AERONAUTICS

WASHINGTON
April 4, 1949

RESTRICTED

UNCLASSIFIED

NATIONAL ADVISORY COMMITTEE FOR AERONAUTICS

RESEARCH MEMORANDUM

EXPERIMENTAL STUDY OF LOOP-SCAVENGED COMPRESSION-IGNITION CYLINDER FOR GAS-GENERATOR USE

By Hampton H. Foster, F. Ralph Schuricht
and Max J. Tauschek

SUMMARY

A preliminary experimental investigation was made of the performance and general operating characteristics of a small ($3\frac{1}{4}$ by $4\frac{1}{2}$ in.) single-cylinder, two-stroke-cycle, loop-scavenged engine using compression ignition at low compression ratios, high inlet-manifold temperatures, and high inlet-manifold and exhaust-gas pressures. The investigation was conducted to determine experimentally the performance characteristics of a ported cylinder for gas-generator use, to compare the results with those obtained by an analysis of a piston-type gas-generator engine, and to indicate the practicability of operating an engine cylinder at the required conditions.

The experimental results, in general, are in reasonable agreement with the performance values analytically obtained for the piston-type burner. Scavenging was unsatisfactory at rich fuel-air mixtures; consequently, the charging efficiency and the power output were somewhat lower than anticipated. The thermal efficiency experimentally determined checked well with analytical results at low fuel-air ratios. Heat losses from the cylinder were inordinately high; these high losses were partly attributed to the high surface-volume ratio of the cylinder and to the low coolant temperature used to expedite the recording of data in this initial investigation. When the heat-rejection rate was considered, the calculated and the measured exhaust-gas temperatures agreed very closely.

Operation of the cylinder at low compression ratios, high inlet-manifold temperatures, high inlet-manifold and exhaust-gas pressures, and high maximum cylinder pressures presented no new problems nor difficulties. Operation was quite smooth because of the low rate of pressure rise in the cylinder.

INTRODUCTION

The potentialities of a gas-generator engine comprising a two-stroke-cycle compression-ignition engine, a compressor, and a turbine are presented in reference 1. In this type of power plant, the piston engine drives its own supercharging compressor and the exhaust gases from the engine are utilized in a turbine, which produces the net useful work of the cycle. A diagrammatic sketch of a gas-generator power plant is shown in figure 1.

Aside from the external operating conditions, the performance of the gas-generator engine is determined by (1) a maximum allowable cylinder pressure, (2) a maximum allowable turbine-inlet temperature, and (3) the necessity that the work output of the piston component of the engine must equal the work requirements of the compressor. In order to satisfy these three conditions simultaneously, compression ratio, manifold pressure, and fuel-air ratio must be adjusted to the proper values. Calculations in reference 1 indicate that compression ratios from 4 to 7, manifold pressures of approximately 80 to 160 pounds per square inch absolute, and over-all fuel-air ratios of approximately 0.03 may be used. The high inlet density results in high air capacity for the gas-generator engine and leads to a low specific engine weight, and the high expansion ratio results in good fuel economy.

The operation of the principal component of this power plant, the two-stroke-cycle compression-ignition engine, is certainly unique and unusual as compared with conventional compression-ignition-engine practice. Consequently, experimental data must be obtained pertaining to the performance of this component and the theory relative to the influence of the rate of combustion-pressure rise on the performance of a pressure- and temperature-limited cylinder; confirmation is also necessary of the theoretical expressions for such items as engine efficiency, heat rejection, compression and combustion pressures, and charging characteristics. An investigation was therefore conducted at the NACA Lewis laboratory to determine experimentally the performance characteristics of a ported cylinder for gas-generator use and to compare the results with those obtained in reference 1.

The unusual operating conditions imposed upon the engine may lead to questions about the mechanical practicability of such an engine. Although a limiting maximum cylinder pressure and exhaust temperature have been maintained, compression ratio, charging pressure and temperature, and exhaust pressure are so far removed from conventional practice that unforeseen mechanical and thermal loads may result in premature engine failure. A careful study of the practicability of operating engine cylinders at these conditions is therefore warranted.

1077

For this work, a small-scale, loop-scavenged, two-stroke-cycle, compression-ignition cylinder was selected as the simplest type of cylinder that was expected to satisfy the gas-generator requirements. This cylinder was operated with compression ratios of 4 to 7, inlet-manifold temperatures ranging from 300° to 600° F, manifold pressures of 80 to 135 pounds per square inch absolute, and over-all fuel-air ratios up to 0.060. The engine speed was held constant at 1800 rpm, and the charge air flow limited to 1 cylinder volume per cycle. Although this engine speed and this rate of flow are not necessarily optimum, the values were selected as the mean between possible limits of the variables (reference 1) in order to limit the number of variables under investigation.

APPARATUS

A ported cylinder with a $3\frac{1}{4}$-inch bore and a $4\frac{1}{2}$-inch stroke was fabricated from steel and the bore was chrome-plated to prevent rapid wear. A detachable cylinder head with various spacers afforded a means of obtaining a change in compression ratio. The inlet- and exhaust-port arrangements were similar to those used by Rogowski and Bouchard (reference 2, fig. 4, section D-D). In this design, two of the eight inlet ports were inclined at an angle of 60° with the base, and the horizontal inlet angles of the other six inlet ports were so arranged as to direct the incoming air upward and toward the inlet side of the cylinder (fig. 2). Four cast-iron piston rings (wedge-shaped cross section) were used above the piston pin; two rings (rectangular cross section) were used below the pin to seal the manifold pressure from the crankcase. A four-plunger pump driven at one-tenth engine speed provided metered lubrication to the cylinder bore at four equally spaced points just above the top of the ports. An oil jet from the small end of the connecting rod was directed at the under side of the crown of the aluminum-alloy piston to cool the piston. The cylinder was mounted on a CFR crankcase. A 100-horsepower dynamometer equipped with the necessary accessories and instrumentation was used to start the engine, to absorb the power, and to motor the engine in order to obtain friction data and compression pressures. The dynamometer torque was indicated by scales. Figures 3 and 4 show general views of the setup.

The fuel-injection pump had a 10-millimeter plunger and a 10-millimeter stroke. The maximum plunger velocity was 0.0125 inch per degree of cam rotation. The spring-loaded injection valve had an opening pressure of 3300 pounds per square inch. Cross sections of the combustion chamber at various compression ratios, the location of the injection valve, and a sketch of the spray pattern are shown

in figure 5. The nozzle used was selected on the basis of a brief preliminary investigation. The fuel had a cetane number of 50, a specific gravity of 0.835 at 60° F, and a hydrogen-carbon ratio of 0.149. Fuel flow was measured with a rotameter.

High-pressure combustion-scavenging air was obtained from the laboratory air system. Weight flow was controlled by suitable valves in the inlet and exhaust systems and was measured by a thin-plate orifice installed according to A.S.M.E. specifications. Surge tanks (figs. 4 and 6) located before and after the engine were equipped with pressure taps to measure the inlet-manifold and exhaust-gas pressures. Maximum cylinder pressures were measured with a balanced-diaphragm valve and a pressure gage. A mercury manometer connected between the inlet manifold and the exhaust tank was used to indicate the pressure drop across the cylinder during operation. The readings were in close agreement with the differences between inlet-manifold and exhaust-gas pressures as indicated by calibrated Bourdon gages.

An electrically operated gas-sampling valve was connected to the combustion chamber from which gas samples were directly piped to a mixture analyzer (reference 3). Samples of gas for a 20° crank-angle period could be obtained for any desired part of the stroke.

During part of this investigation, the engine was operated on a four-stroke cycle, that is, with fuel injection at the end of every second compression stroke in order to insure the removal of unburned fuel from the cylinder prior to the air-charging process. This operation was accomplished by the use of 2:1 reduction gear between the engine and the fuel-injection pump.

Indicator-card (pressure-time diagrams) data were obtained with a modified Farnboro electric indicator (reference 4).

PROCEDURE

Variable fuel-air-ratio runs were made over a range of inlet-manifold pressures and corresponding exhaust-gas pressures, so that the chosen scavenging ratio (ratio of volume of air flowing through the cylinder per cycle measured at inlet-manifold conditions to the volume of the cylinder at the time of port closing) was constant. The inlet-air flow was controlled by throttling the flow of exhaust gases. The engine speed was held constant by varying the load on the dynamometer for changes in fuel-air ratio; the fuel-injection advance angle was also held constant.

1077

1077

Data were recorded at a minimum of 15-minute intervals to permit stabilization of operating temperatures. Friction losses were determined by motoring the engine after each point at which data were taken.

The following engine operating conditions were used:

Port timing, deg A.T.C.	
Exhaust opens	109
Exhaust closes	251
Inlet opens	119
Inlet closes	241
Compression ratios (based on volume above exhaust ports)	4, 4.5, 5.25, and 7
Engine speed, rpm	1800
Inlet-manifold pressures, lb/sq in. abs.	80, 100, 120, and 135
Injection-advance angle, deg	25
Fuel-air-ratio (over-all) range	0.01 to 0.060
Inlet-manifold temperature, $^{\circ}F$	300, 400, 500, and 600
Coolant inlet temperature, $^{\circ}F$	165

RESULTS AND DISCUSSION

Scavenging Characteristics

Port flow coefficients. - Flow coefficients of the inlet and exhaust ports were determined under steady-flow conditions. The air flow through the cylinder was measured at successive positions of the piston, which controlled the port openings. The inlet- and exhaust-flow coefficients based on the maximum port areas are shown in figure 7(a). The average steady-flow coefficients based on maximum port area were found to be 0.238 and 0.372 for the inlet and exhaust systems, respectively. Figure 7(b) shows a plot of the products of the values of open-port areas and the corresponding values of discharge coefficient at different crank positions in the scavenging period. The average values of this product are 0.653 and 0.923 square inch for the inlet and exhaust systems, respectively.

A parameter M, first developed for an analysis of the flow through poppet valves (reference 5) was modified for use in the study of flow through a ported cylinder and was used to compare the inlet and exhaust systems of the ported cylinder with those of a cylinder from a 12-cylinder conventional aircraft engine. The value of M (designated ϕ in reference 5) is a dimensionless number representing the hypothetical average Mach number for the flow through the valves or ports when the piston is assumed to induct or exhaust

the charge at a constant pressure. (See appendix for method of calculation of M.) Although the flow processes do not actually occur in this manner, this assumption permits a convenient method or index for comparing the capacities of various valve systems, inasmuch as it takes into account the valve areas, the rates of opening, the flow coefficients, the total opening periods, and the cylinder dimensions. With this method of comparison, the lower the value of M, the greater the capacity of the valve under the operating conditions considered. The comparative values of M for the ported cylinder and the cylinder of a conventional aircraft engine at piston speeds of 1350 and 2400 feet per minute and arbitrarily chosen inlet and exhaust sonic velocities of 1100 and 2500 feet per second, respectively, are:

	Ported cylinder	Conventional aircraft-engine cylinder
Engine speed at piston speed of 1350 feet per minute	1800 rpm	1350 rpm
Inlet M	0.344	0.144
Exhaust M	0.098	0.088
Engine speed at piston speed of 2400 feet per minute	3267 rpm	2400 rpm (rated)
Inlet M	0.624	0.263
Exhaust M	0.179	0.160

The relatively high, and therefore unfavorable, values of M for the inlet ports are due to the angular arrangement, the length of the flow passages, and the sharp edges at the entrances of the ports (fig. 2).

Cylinder pressure drop. - Typical cylinder-pressure-drop data obtained during the investigation are shown in figure 8. The pressure drops shown here range from approximately 4 to 23 pounds per square inch and vary with manifold pressure and fuel-air ratio.

These data may be compared with calculated values of pressure drop for the ported cylinder and also for the cylinder of references 1 and 2, which were calculated by means of the equation used in the previous analysis (reference 1):

$$R_s = 0.0910 \sqrt{\left(1 - \frac{p_e}{p_m}\right) T_m} \qquad (1)$$

1077

where

R_s scavenging ratio

p_e exhaust-gas pressure, (lb/sq in. abs.)

p_m inlet-manifold pressure, (lb/sq in. abs.)

T_m inlet-manifold temperature, ($^\circ$R)

This equation was intended to apply to cruising engine speeds corresponding to a mean piston speed of approximately 1800 feet per minute. The experimental cylinder, however, was operated at a mean piston speed of 1350 feet per minute. If the cylinder and the ports are assumed to have the characteristics of an orifice and the weight flow is assumed directly proportional to the average piston speed, the cylinder pressure drop will vary as the square of the average piston speed. Consequently, equation (1) becomes

$$p_m - p_e = \left(\frac{R_s}{0.0910}\right)^2 \left(\frac{1350}{1800}\right)^2 \frac{p_m}{T_m} \qquad (2)$$

Pressure drops calculated from equation (2) are compared with the experimental data for a fuel-air ratio of 0.03 in figure 9. The differences between the calculated and experimental data are in a large part attributed to the low inlet-port flow coefficients and the inadequate exhaust lead of the cylinder under investigation. Because the analytical expression is independent of fuel-air ratio, the pronounced effect of fuel-air ratio on the pressure drop across the experimental cylinder (as illustrated in fig. 8) is further evidence of inadequate exhaust lead or time-area for the exhaust blowdown process. The required exhaust lead, determined by a method presented in reference 6, was about six times that of the experimental cylinder.

Charging efficiency. - In reference 1 it is assumed that perfect mixing accompanies the charging process (reference 6). For this scavenging process, the charging efficiency η_s is given by reference 7 as

$$\eta_s = 1 - e^{-R_s} \qquad (3)$$

At the selected operating condition, that is, a scavenging ratio of unity, the charging efficiency from equation (3) is 63.2 percent. Samples of gas from the experimental cylinder, however, indicated that the charging efficiency was less than 55 percent, which represents a loss of 13 percent in power output at rich mixtures.

For operation at over-all fuel-air ratios in excess of 0.035, experimental data indicate that as the fuel-air ratio is enriched the charging efficiency decreases and ultimately approaches zero. This relation is caused by the cylinder fuel-air ratio being stoichiometric or richer so that all the fuel cannot burn. When the scavenging process begins, the unburned fuel remaining from the previous cycle apparently undergoes combustion, using part of the scavenge air. As a result, the cylinder is in part being scavenged with products of combustion. On succeeding cycles, the cylinder fuel-air ratio becomes increasingly richer until equilibrium is reached, at which time the concentration of products of combustion in the cylinder is very high at inlet-port closure.

The effect of high concentration of the products of combustion is demonstrated by the data of figure 10. The indicated mean effective pressure decreases rather rapidly as the cylinder fuel-air ratio goes beyond stoichiometric, corresponding to an over-all fuel-air ratio of about 0.035, which is indicative of the poor scavenging under these operating conditions. The burning of practically all the fuel during some part of the cycle, whether it is during the power stroke or during the initial stages of the scavenging process, is clearly illustrated by the curve of exhaust-gas temperature, which continues to increase with increasing over-all fuel-air ratio.

Operation on a four-stroke cycle (with fuel injection every other cycle) should demonstrate the effect of the unburned fuel that exists in the cylinder at the beginning of scavenging. In this case, the unburned fuel and products of combustion resulting from burning during the scavenging period are carried out of the cylinder on the nonfiring cycle. The power curve as a function of fuel-air ratio therefore should not peak but should become substantially flat as the cylinder fuel-air ratio becomes richer than stoichiometric. The four-stroke-cycle data, shown only in figure 10, confirm this conclusion.

Power Output

Effect of engine operating conditions. - The effect of inlet-manifold temperature, inlet-manifold pressure, and fuel-air ratio on the indicated mean effective pressure of the experimental cylinder is shown in figures 11 and 12.

At very lean fuel-air ratios (below 0.025), figure 11 indicates that the indicated mean effective pressure is roughly proportional to the fuel flow. As the mixture is enriched, the slope of the curve decreases and ultimately reaches a value of zero. This point corresponds to approximately stoichiometric mixture in the cylinder, which is approximately twice the over-all fuel-air ratio for the chosen operating conditions and resultant charging efficiency.

For changes in inlet-manifold pressure or inlet-manifold temperature, the data of figures 11 and 12 show upon analysis that the indicated mean effective pressure is almost directly proportional to the density of the air in the inlet manifold. This proportionality is a natural result of the manner in which the operating conditions were changed inasmuch as the air flow was held constant at 1 cylinder volume per cycle. Small changes in charging and thermal efficiencies occurring through changes in manifold conditions caused slight variations from this relation.

Comparison with calculated results. - The power output from the experimental cylinder cannot be directly compared with that calculated in the analysis (reference 1) because the combustion pressure rise used in the analysis was considerably greater than that experimentally found. A valid comparison between the calculated and experimental power results may be made, however, if the inlet-manifold pressure is kept constant and the results are compared at the same values of maximum cylinder pressure and exhaust-gas temperature, the two limiting factors in the gas-generator engine. Such a comparison is shown in figure 13 for values of mean effective pressure calculated according to thermodynamic relations shown in reference 1 for equivalent values of experimental maximum cylinder pressure and corresponding exhaust-gas temperatures. The results are in fair agreement at conditions of low exhaust temperature, which correspond to lean fuel-air ratios (less than 0.03). Optimizing the injection advance angle may improve the agreement here by increasing the power output and also decreasing the cylinder pressure and the exhaust temperature. At conditions corresponding to rich fuel-air ratios, wide differences are noted between the calculated and experimental values. Most of the difference is attributed to the poor charging efficiency of the experimental cylinder, although injection advance, duration, and pattern also exert some influence on the power output.

Cylinder Pressures

Compression pressures. - A comparison of calculated and experimental compression pressures is shown in figure 14. The expression used in the reference analysis (reference 1),

$$p_c = p_e r^{1.35} \quad (4)$$

where

p_c compression pressure, (lb/sq in. abs.)

p_e exhaust-gas pressure, (lb/sq in. abs.)

r compression ratio

is shown to result in pressures somewhat lower than the actual compression pressures. In view of the low flow coefficient across the inlet ports of the experimental cylinder, it appears doubtful that compression could proceed from inlet-manifold pressure. Actually, the pressure from which compression begins should be somewhere between inlet- and exhaust-manifold pressures. Indicator-card data show that this pressure is less than the inlet-manifold pressure by about 20 percent of the cylinder pressure drop. The data in figure 14 show that the value of 1.35 for the polytropic exponent very nearly fits the plotted points.

Maximum cylinder pressures. - The effect of inlet-manifold pressure and fuel-air ratio on maximum cylinder pressure is shown in figure 15. The curves initially rise quite rapidly and, as the fuel-air ratio is enriched, become more nearly flat. This flatness is a result of increasing the duration of fuel injection at the richer mixtures and of operating with a fixed injection advance angle. If the injection advance had been optimized, increasing with the fuel-air ratio, these curves would be more nearly straight lines. As is to be expected, the maximum cylinder pressure at a given fuel-air ratio is approximately proportional to the inlet-manifold pressure.

Ratios of maximum combustion pressures to compression pressure are plotted in figure 16 for both experimental and calculated values of cylinder pressure. The calculated values were obtained by using the method of computation (for constant-volume combustion with certain correction factors applied) described in the analysis (reference 1). The calculated values of combustion pressure are higher than the experimental values and the calculated values of compression pressures $p_e r^{1.35}$ are slightly lower than the experimental values, being nearly $p_m r^{1.35}$. Thus the calculated ratios are accordingly higher than the experimental ratios. The pressure

1077

ratio increases as the compression ratio is decreased. For example, the value of the experimental pressure ratio for a compression ratio of 7 is 1.42 whereas for a compression ratio of 4 it is 1.72 (at a fuel-air ratio of 0.035).

At high compression ratios, the temperature is, of course, higher at the end of compression than at low compression ratios. This increase in temperature caused the decrease in the ratio of combustion pressure to compression pressure with increasing compression ratio (fig. 16) for the calculated data and is a contributing factor in accounting for this variation in the case of the experimental data. For the experimental data, however, a second effect is present, because combustion is incomplete at crank top dead center and because the rate of change of cylinder volume with respect to time for constant clearance volume is greater for high than for low compression ratios.

The combustion pressure rise was about one-half of that to be expected with constant-volume combustion. The combustion pressure rise apparently had little bearing on the performance of the cylinder when the limitations were maximum cylinder pressure and exhaust-gas temperature.

Thermal Efficiency

The effects of pertinent engine operating variables on indicated specific fuel consumption and thermal efficiency of the experimental cylinder are shown in figure 17, which shows that the efficiency decreases with increasing fuel-air ratio. This change is caused by the greater divergence of the properties of the working fluid from the properties of a perfect gas at the rich mixtures, the occurrence of more of the combustion process at constant pressure, and the burning of some fuel at bottom center, as previously discussed. In addition, these values include a combustion efficiency, which was not determined but was estimated to be approximately 90 to 100 percent.

The variation of thermal efficiency with compression ratio is compared to that of an air standard cycle in figure 18. The trend of the experimental data is shown to be similar to that expected from theoretical considerations.

The experimental data are compared with the efficiencies calculated by the methods of the reference analysis (reference 1) in figure 19. The figure shows that the experimental values are somewhat less than the theoretical results. In the course of the investigation,

1077

time did not permit optimizing injection pattern, injection advance, or duration of injection. Furthermore, some loss in efficiency can be attributed to the low charging efficiency. For these reasons, the data of figure 19 are considered to be a reasonable check on the assumptions in the initial analysis, particularly at fuel-air ratios less than 0.03.

Exhaust Measurements

Heat losses. - The heat loss to the coolant and the exhaust-gas temperature of the experimental cylinder are shown in figure 20 as functions of fuel-air ratio. The heat losses decrease with an increase in fuel-air ratio. This variation probably results because the heat input increases faster than the temperature difference leading to heat transfer. All the data are considerably higher than the value of 18 percent assumed in the previous analysis (reference 1). The higher heat rejection of the experimental cylinder is partly attributed to the high surface-volume ratio of this cylinder (the experimental cylinder has a surface-volume ratio over $2\frac{1}{2}$ times that of a 6.3- by 6.3-in. loop-scavenged two-stroke-cycle cylinder (Klöckner Humbolt Deutz engine, reference 8)), and partly to the low coolant temperature used to expedite the investigation.

Exhaust-gas temperature. - The exhaust-gas temperature (fig. 20) is practically a linear function of fuel-air ratio. The slight amount of upward curvature is caused by a decrease in the engine efficiency as the fuel-air ratio is increased. The difficulty of attaining equilibrium conditions in the exhaust tank, which had considerable thermal lag, may account for the scatter in the data points. Because the data were taken in the direction of increasingly rich mixtures, the higher temperatures at each respective fuel-air ratio are considered most valid and the line through the points is drawn accordingly.

Comparison of calculated and experimental exhaust-gas temperatures. - The equation used in the previous analysis (reference 1) was modified to eliminate the necessity for knowing the compressor-inlet temperature in the gas-generator engine, to eliminate the simplifying assumption of constant specific heat, and to consider the higher heat losses in the experimental cylinder. In its modified form, the equation becomes

$$H_g = \frac{(1 - Q_l - \eta_t)\, h_c \left(\frac{F}{A}\right)}{\left(1 + \frac{F}{A}\right)} + H_m \qquad (5)$$

1077

where

H_g enthalpy of exhaust gas, Btu per pound

Q_l heat rejection, fraction of heat input neglecting friction

η_t indicated thermal efficiency from experimental data

h_c heat of combustion of fuel, 18,500 Btu per pound

F/A fuel-air ratio

H_m enthalpy of inlet air, Btu per pound

Data from reference 9 allowed graphical expression of these enthalpy values as functions of temperature and fuel-air ratio and thus permitted a solution of the equation to be made. Equation (5) results in the same exhaust-gas temperature as that calculated in the analysis in reference 1 for a corresponding heat-rejection rate.

Values of exhaust-gas temperature calculated by means of equation (5) are compared with the experimentally determined values in figure 21. The calculated values appear to be in good agreement with the experimental results. At a fuel-air ratio of 0.04 and beyond, all the data points lie below the calculated curves. This disparity may be a result of decreasing combustion efficiency in the experimental data because the equations assume 100-percent combustion efficiency, or of neglected heat losses at the high temperatures involved.

The variation in calculated and experimental exhaust-gas temperatures with changes in compression ratio is shown in figure 22. Here again the correlation is shown to be good. The change in exhaust-gas temperature with compression ratio is caused by variation in the thermal efficiency of the cylinder.

EFFECT OF DIFFERENCES BETWEEN OBSERVED AND PREDICTED PERFORMANCE

Inasmuch as this investigation was conducted to determine experimentally the performance characteristics of a cylinder for gas-generator use and to compare the data obtained with those assumed for the previous analysis of the gas generator (reference 1), examination of the effect of differences in the experimental and assumed data on the performance of the gas-generator engine is of interest.

1077

The two most serious deficiencies of the experimental cylinder with regard to gas-generator application are its low charging efficiency and its high heat losses. The low charging efficiency causes a loss in power output, which may limit the manifold pressure at which the gas-generator engine can operate. This limitation in turn leads to higher specific weight and specific fuel consumption in the gas-generator engine.

The nature of this power limit is shown in figure 23. The cylinder power output is shown for constant exhaust-gas temperature and constant maximum cylinder pressure. The operating point of the gas-generator engine obviously is that point where the power-available curve intersects the power-required curve. Because all the curves are so nearly parallel, a small drop in power output resulting from inadequate scavenging results in a large loss in manifold pressure.

The gas-generator engine ordinarily operates at fuel-air ratios of about 0.03 to 0.035 and if the scavenging is adequate to keep the cylinder fuel-air ratio somewhat below stoichiometric, complete scavenging is no longer so important. The present cylinder is incapable of accomplishing this end. Revision of the porting scheme with particular emphasis on increasing the exhaust lead may effect a satisfactory improvement.

The second fault of the present cylinder, that of excessive heat losses, is attributed to the use of a small-scale cylinder with a low coolant temperature. In this investigation, overcooling the cylinder rather than developing a cylinder that would operate well with a minimum of cooling was expedient. The use of a full-scale cylinder with a certain amount of development to permit the use of higher coolant temperatures should be effective in reducing the heat losses. A reduction of manifold cooling area would also be made possible with a full-scale cylinder. Despite poor scavenging and high heat losses, the performance of the experimental cylinder confirmed the assumptions used in the previous analysis sufficiently well to indicate that a reasonable approach could be made to the gas-generator-engine performance calculated in reference 1.

MECHANICAL PERFORMANCE OF ASSEMBLY

The operating conditions used in the investigation represent quite a radical departure from conventional practice. Accordingly, the practicability of operating at these conditions may be questioned.

Many of the anticipated difficulties, such as, roughness of the engine, broken and stuck piston rings, broken cylinders, connecting rods, and pistons, and rapid wear of parts failed to materialize. The engine operated satisfactorily throughout the entire investigation. Ring sticking was not a problem, nor was combustion roughness or knock encountered. The average rate of combustion-pressure rise was 32.5 pounds per square inch per degree at 1800 rpm or 352,000 pounds per square inch per second as determined from indicator cards. A minimum rate of pressure rise of about 50 pounds per square inch per degree will usually cause engine roughness. It should be pointed out, however, that no attempt has been made to reduce the high heat losses from the cylinder; the higher cylinder temperatures that would accompany such an attempt have not been investigated.

SUMMARY OF RESULTS

The results of an investigation of the performance of a small-scale, two-stroke-cycle, compression-ignition cylinder of the loop-scavenged type operated under simulated piston-type gas-generator-engine conditions may be summarized as follows:

1. Charging and scavenging of the cylinder was inadequate because of unsatisfactory porting. The poor charging and scavenging were traced to inadequate exhaust lead, which was found to be only one-sixth of that required. The charging efficiency adversely affected power output and thermal efficiency of the cylinder at over-all fuel-air ratios in excess of 0.03.

2. The thermal efficiency and the power output at over-all fuel-air ratios less than 0.03 checked satisfactorily with anticipated values. Small improvements may be obtained by optimizing the fuel-injection-system characteristics.

3. Heat losses from the cylinder were excessive. Part of the reason for these large losses was the necessarily large surface-volume ratio of the cylinder, which was about $2\frac{1}{2}$ times that of a current full-scale two-stroke-cycle cylinder. A contributing factor was the low coolant temperature used to expedite the investigation.

4. Measured exhaust-gas temperatures checked anticipated values reasonably well when the experimentally determined heat losses and combustion efficiency were considered.

5. The combustion pressure rise was about one-half that to be expected with constant-volume combustion. The combustion pressure

rise apparently had little bearing on the performance of the cylinder when the limitations were maximum cylinder pressure and exhaust-gas temperature.

6. An analysis of the data showed that inadequate cylinder charging (charge air insufficient to maintain the cylinder fuel-air ratio somewhat below stoichiometric) limited the manifold pressure at which a gas-generator engine using this cylinder may operate. The analysis indicates, however, that if the cylinder charging was adequate, only small increases in allowable manifold pressure would accompany further improvement in charging efficiency.

7. The unusual operating conditions had no harmful effects on the mechanical operation of the engine; the operation was quite smooth because of the low rate of combustion-pressure rise in the cylinder.

Lewis Flight Propulsion Laboratory,
National Advisory Committee for Aeronautics,
Cleveland, Ohio.

APPENDIX - METHOD OF COMPUTING COMPARISON PARAMETERS FOR INLET AND EXHAUST SYSTEMS

When an amount of air equal to the piston displacement is assumed to flow through the valves at constant pressure during the inlet and exhaust processes, let $A_{max}C_a$ be the product of maximum valve or port area and average flow coefficient based on that area, in square inches.

Then

$$\rho(A_{max}C_a)\ Vt = \frac{\rho v_D}{12}$$

$$V = \frac{v_D}{12(A_{max}C_a)t}$$

but

$$t = \frac{\Delta\theta}{6N}$$

$$V = \frac{v_D N}{2(A_{max}C_a)\Delta\theta}$$

and

$$\frac{V}{c} = M = \frac{v_D N}{2c(A_{max}C_a)\Delta\theta}$$

but

$$v_D N = 12\,\frac{S}{2}\,A_p$$

so that

$$M = \frac{3SA_p}{c(A_{max}C_a)\Delta\theta}$$

where

ρ fluid density, lb/cu ft

V average velocity of flow through valves or ports, ft/sec

t time for flow process, sec

v_D piston displacement, cu in.

$\Delta\theta$ total valve- or port-opening period, deg

N engine speed, rpm

c velocity of sound (1100 ft/sec at inlet conditions, 2500 ft/sec at exhaust conditions, values arbitrarily chosen)

M hypothetical average Mach number for flow through valve or port

S average piston speed, ft/min

A_p area of piston, sq in.

The data necessary for determining the values of M for the ported and for the conventional aircraft-engine cylinder and also comparative values of M for each are as follows:

Concept	Ported cylinder		Aircraft-engine cylinder	
	Inlet	Exhaust	Inlet	Exhaust
S, (ft/min)	1350	1350	1350	1350
A_p, (sq in.)	8.3	8.3	23.7	23.7
c, (ft/sec)	1120	2500	1120	2500
A_{max}(total), (sq in.)	3.03	2.62	5.16	4.15
C_a	0.238	0.372	0.398	0.373
$\Delta\theta$, deg	122	142	290	282
M	0.344	0.0985	0.144	0.088
M (2400 rpm[a])	0.624	0.179	0.263	0.160

[a]Rated speed for aircraft-engine cylinder.

REFERENCES

1. Tauschek, Max J., and Biermann, Arnold E.: An Analysis of a Piston-Type Gas-Generator Engine. NACA RM No. E7I10, 1948.

2. Bogowski, A. R., and Bouchard, C. L.: Scavenging a Piston-Ported Two-Stroke Cylinder. NACA TN No. 674, 1938.

3. Gerrish, Harold C., Meem, J. Lawrence, Jr., Scadron, Marvin D., and Colnar, Anthony: The NACA Mixture Analyzer and Its Application to Mixture-Distribution Measurement in Flight. NACA TN No. 1238, 1947.

1077

4. Collins, John H., Jr.: Alterations and Tests of the "Farnboro" Engine Indicator. NACA TN No. 348, 1930.

5. Stanitz, John D.: An Analysis of the Factors That Affect the Exhaust Process of a Four-Stroke-Cycle Reciprocating Engine. NACA TN No. 1242, 1947.

6. Schweitzer, P. H.: Porting of Two-Stroke Cycle Diesel Engines - Pt. II. Diesel Power & Diesel Transportation, vol. 20, no. 6, June 1942, pp. 477-479.

7. Taylor, C. Fayette, and Taylor, Edward S.: The Internal Combustion Engine. International Textbook Co. (Scranton, Pa.), 1938, pp. 240-255.

8. Pope, Arthur W., Jr.: KHD Two Cycle Engine Developments with Schnuerle Loop Scavenge System. Fiat Final Rep. No. 683, Off. Director of Intell., U. S. Office Military Govt. (Germany), Jan. 9, 1946. (Available from U. S. Dept Commerce as PB No. 30041.)

9. Pinkel, Benjamin, and Turner, L. Richard: Thermodynamic Data for the Computation of the Performance of Exhaust-Gas Turbines. NACA ARR No. 4B25, 1944.

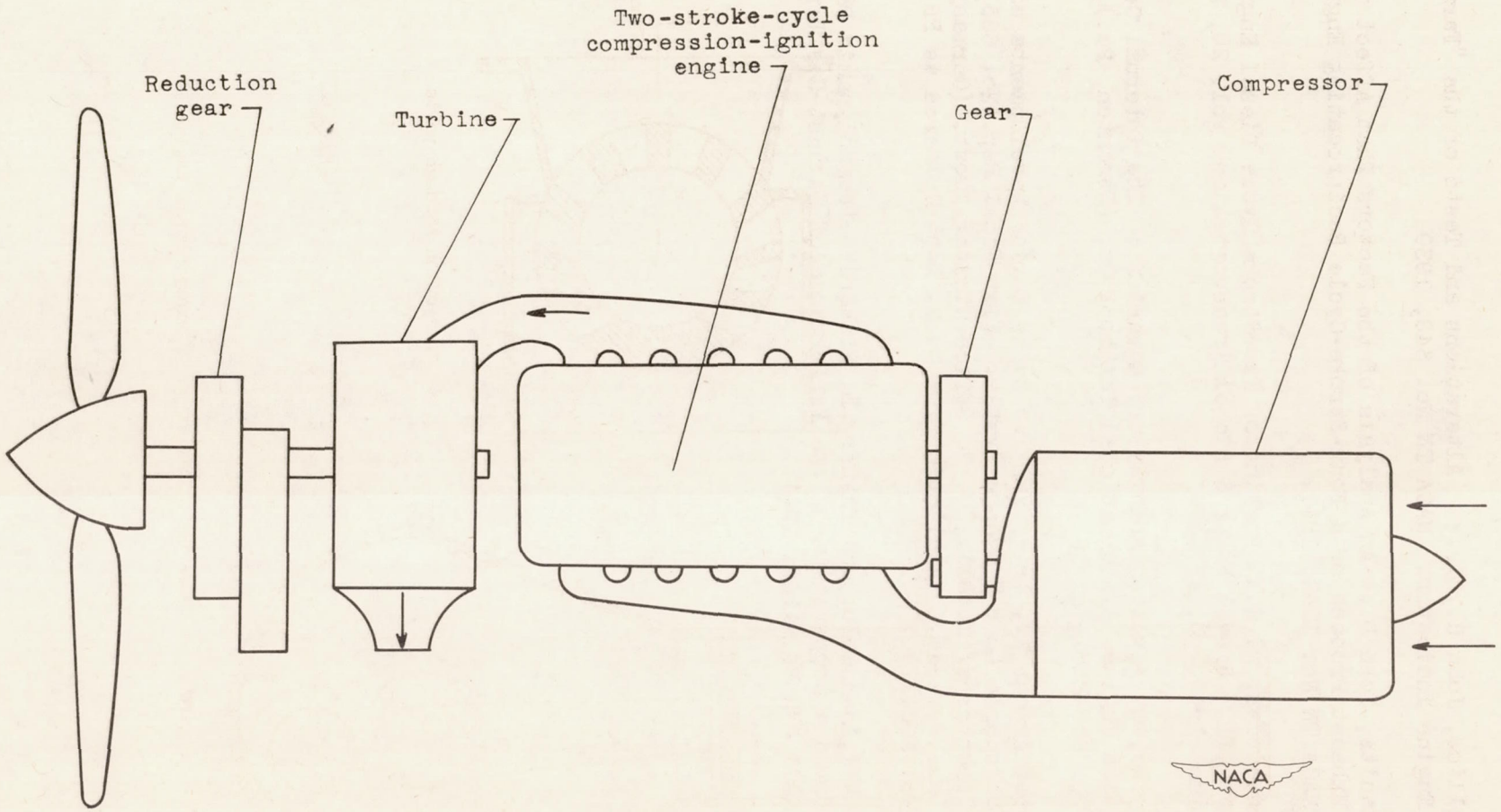
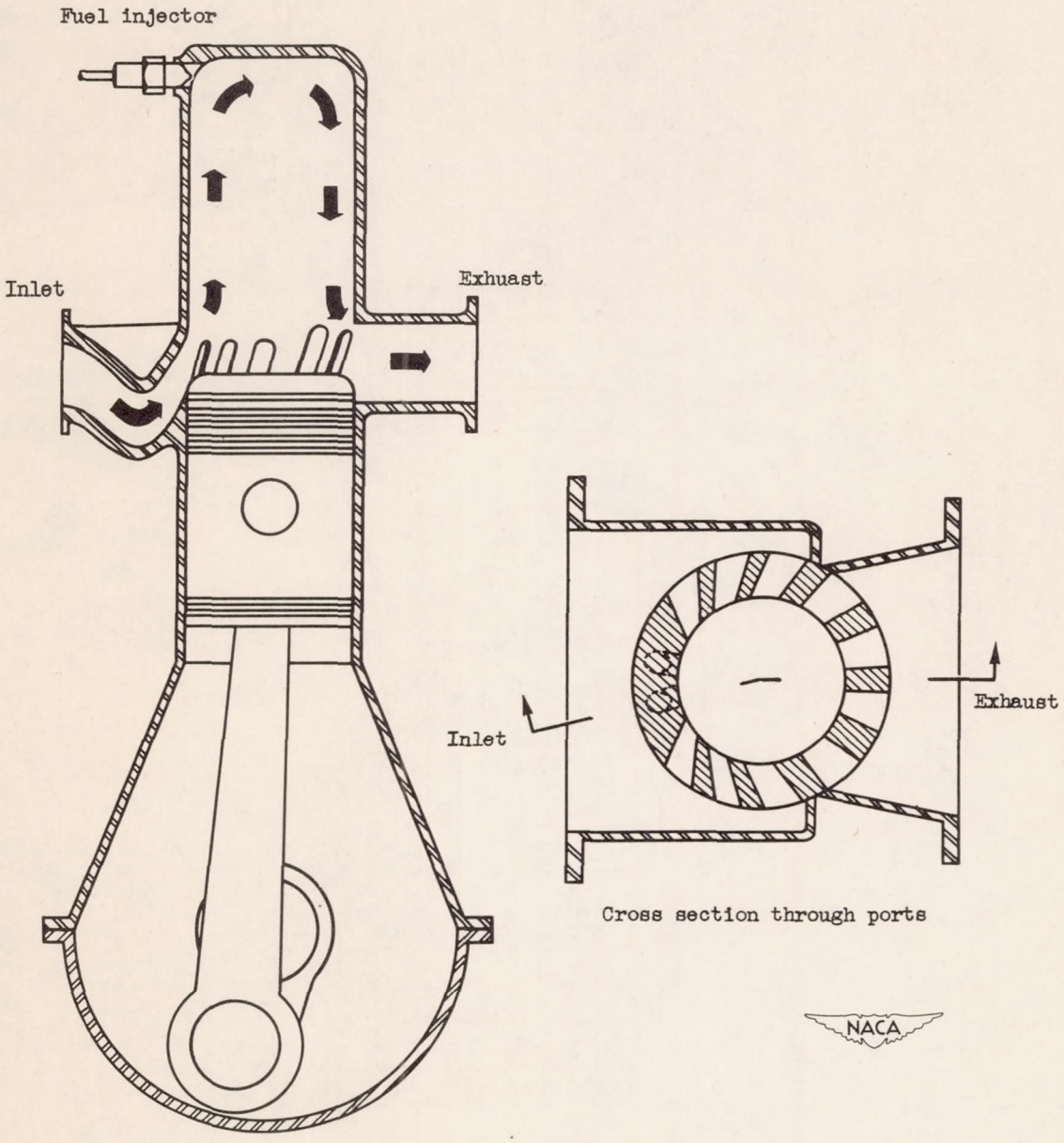


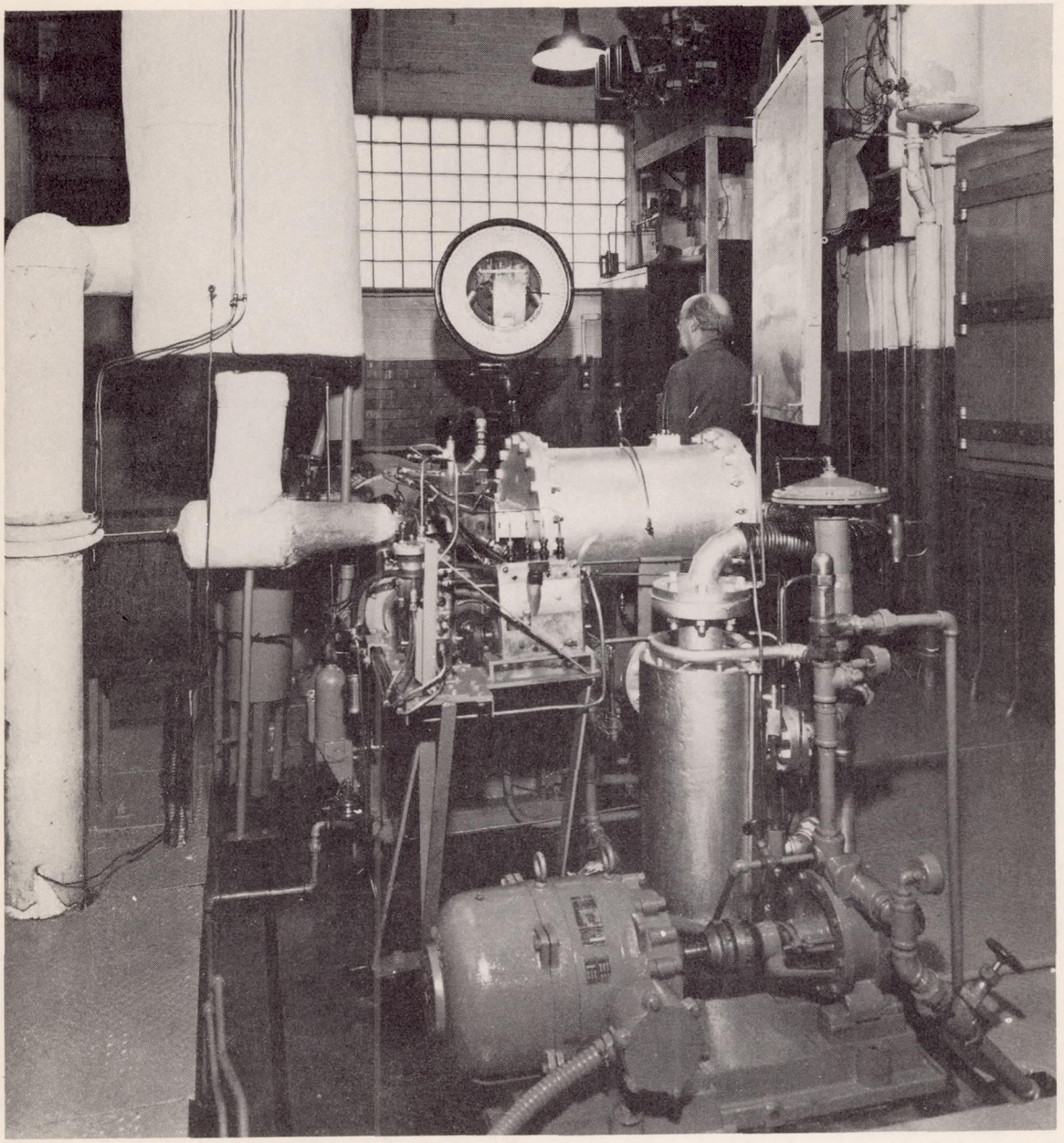
Figure 1. - Diagrammatic sketch of gas-generator engine used in analysis (reference 1).

1077



154-987-A

Figure 2. - Cross-sectional views of experimental engine.



NACA
C-20857
3-1-48

Figure 3. - General view of engine setup.

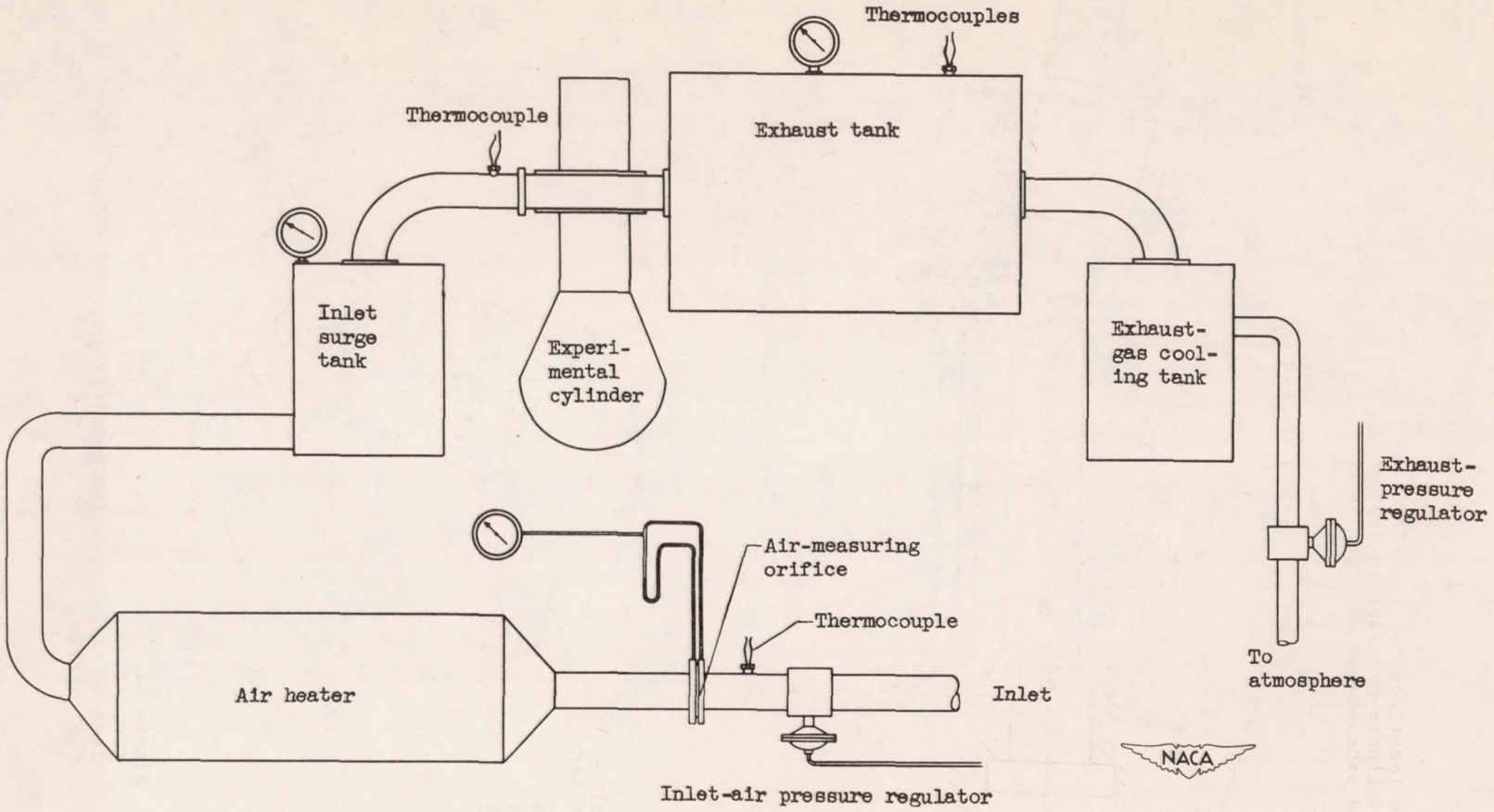
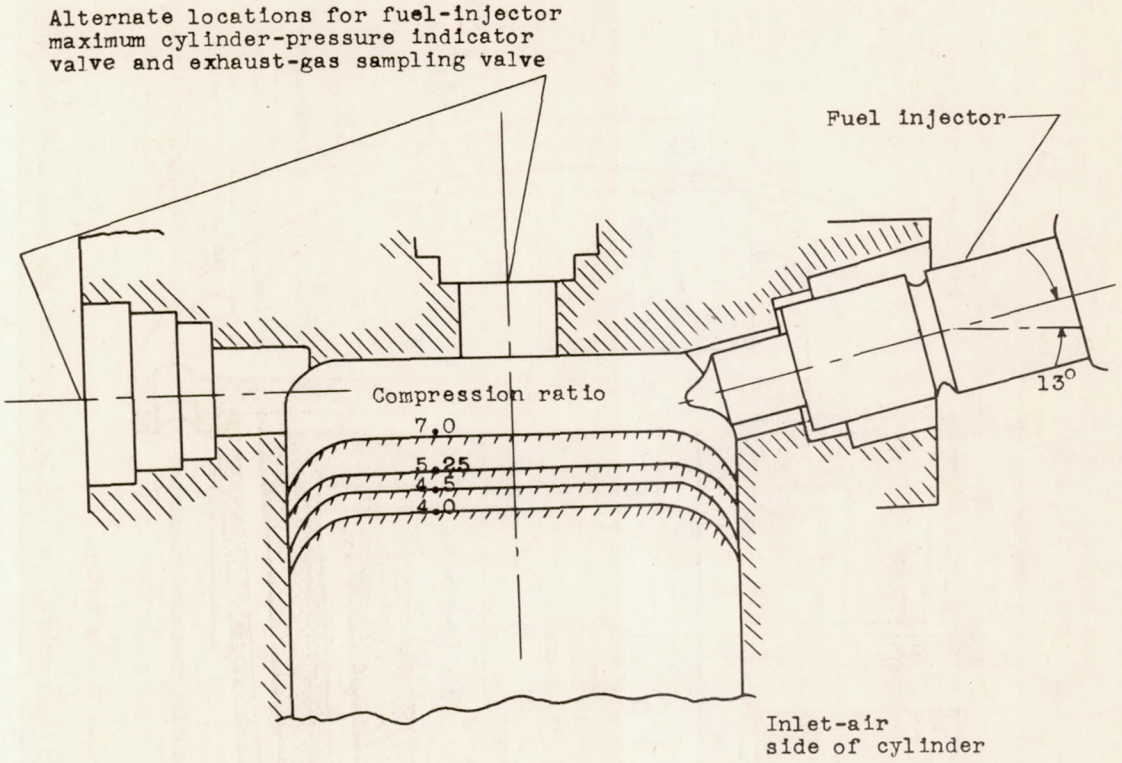


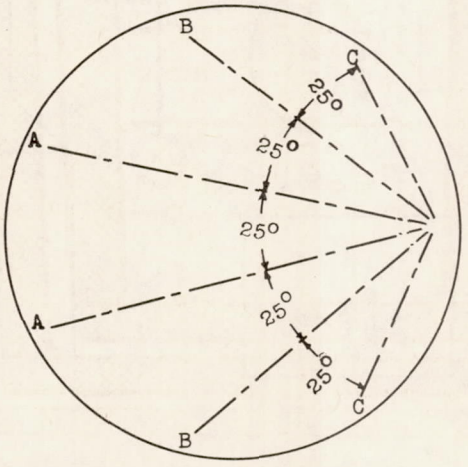
Figure 4. - Engine setup.

1077



Fuel-nozzle-orifice diameters (in.)

A	0.019
B	.014
C	.008



Section through plane of sprays

Figure 5. - Outlines of combustion chamber (for compression ratios of 4, 4.5, 5.25, and 7), location of fuel-injection valve, and pattern of fuel sprays.

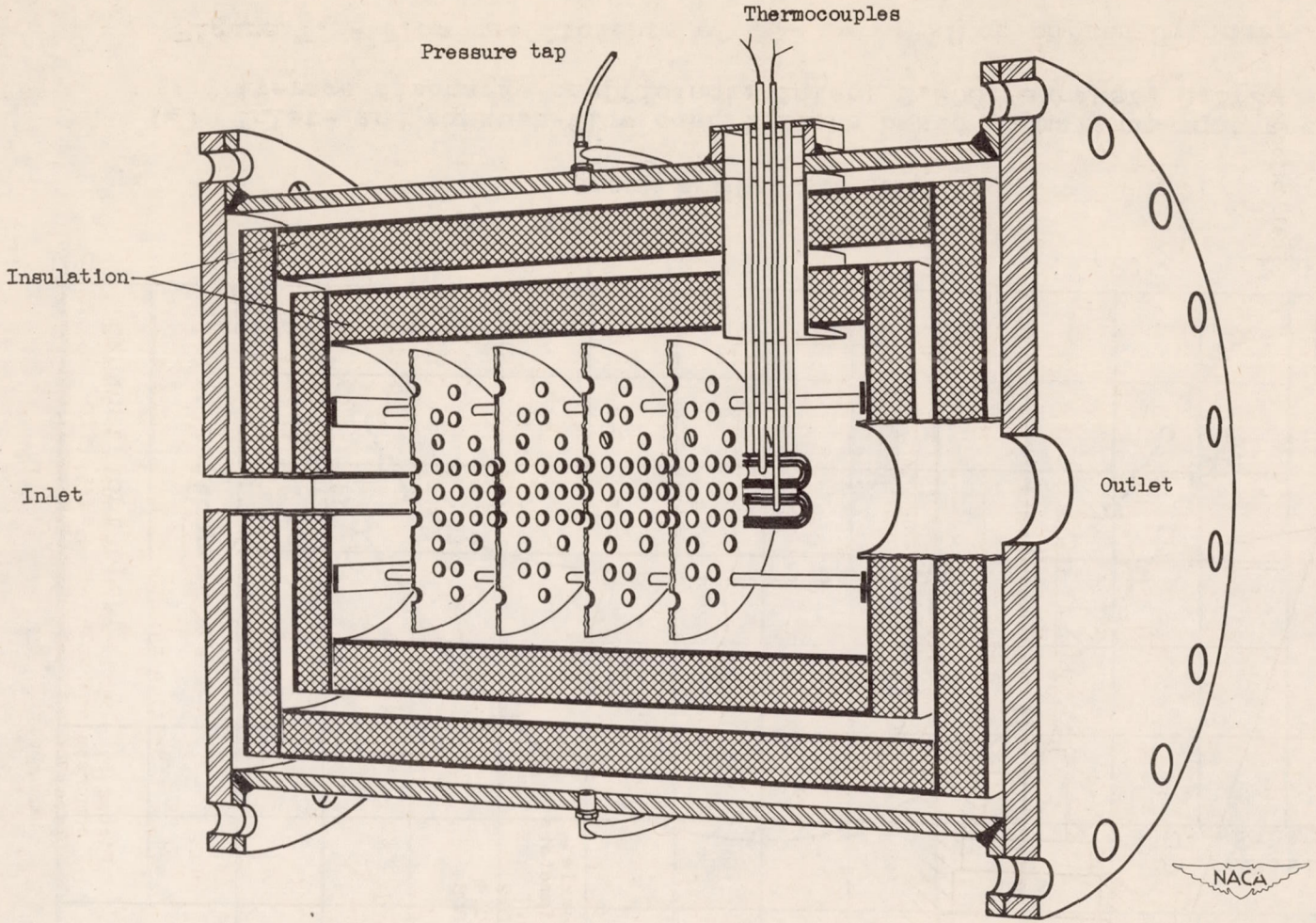
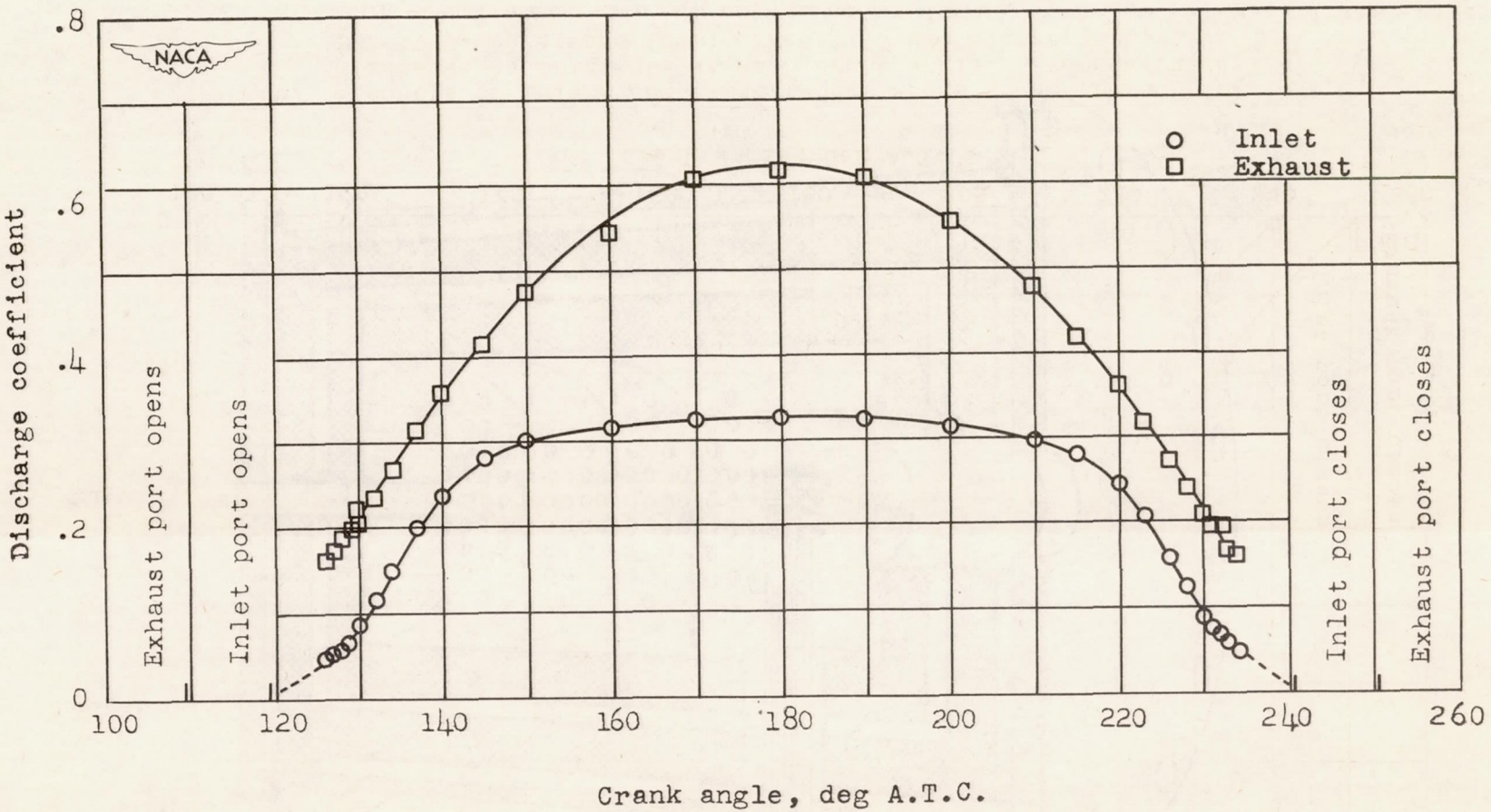
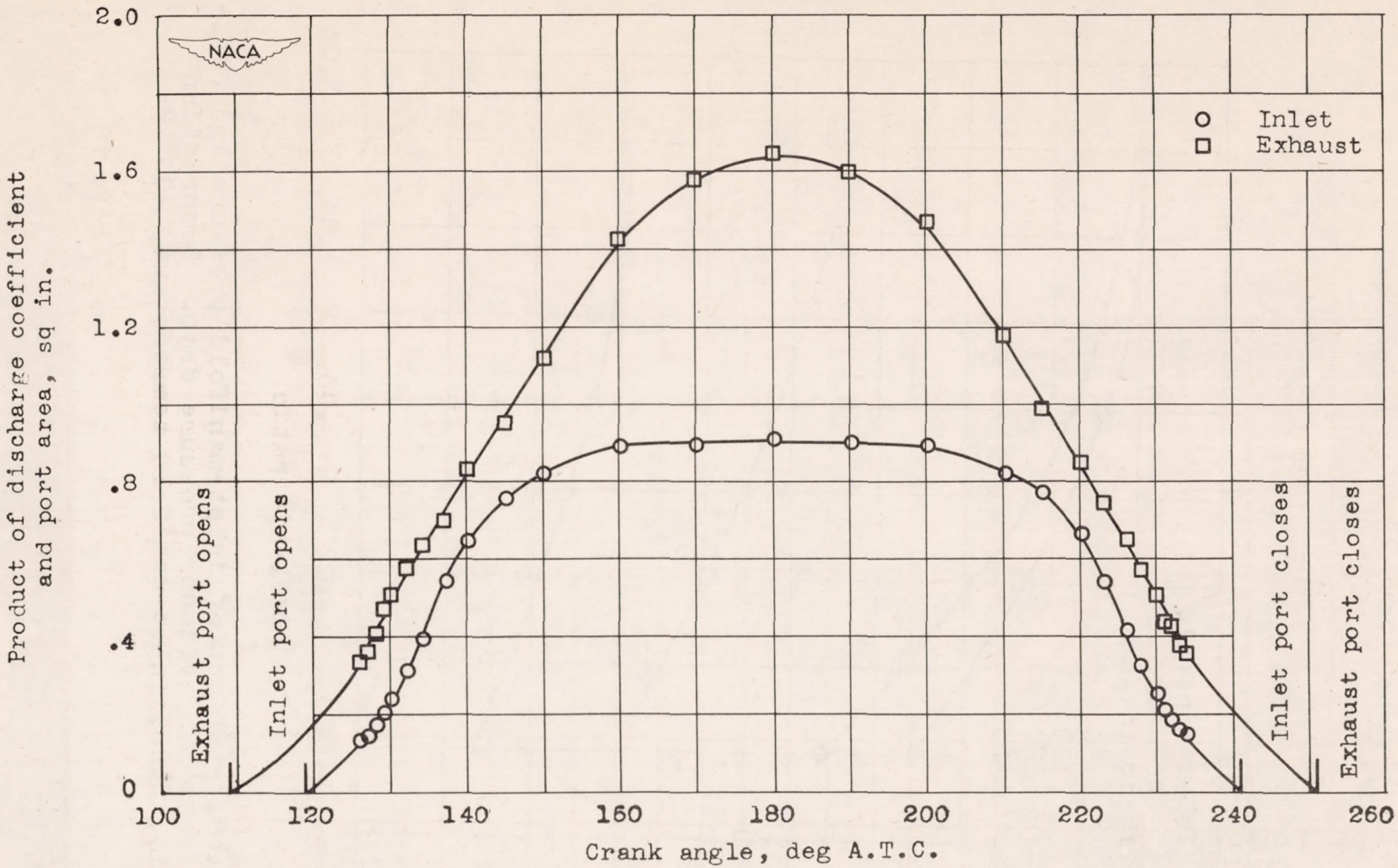


Figure 6. - Longitudinal section through exhaust surge tank instrumented for obtaining exhaust-gas pressures and temperatures.



(a) Inlet- and exhaust-flow coefficients based on maximum port area. Average discharge coefficient: inlet, 0.238; exhaust, 0.372.

Figure 7. - Flow coefficients of $3\frac{1}{4}$- by $4\frac{1}{2}$-inch ported cylinder.



(b) Products of inlet- and exhaust-port areas and corresponding discharge coefficients at each crank angle. Average values: inlet, 0.653 square inch; exhaust, 0.923 square inch.

Figure 7. - Concluded. Flow coefficients of $3\frac{1}{4}$- by $4\frac{1}{2}$-inch ported cylinder.

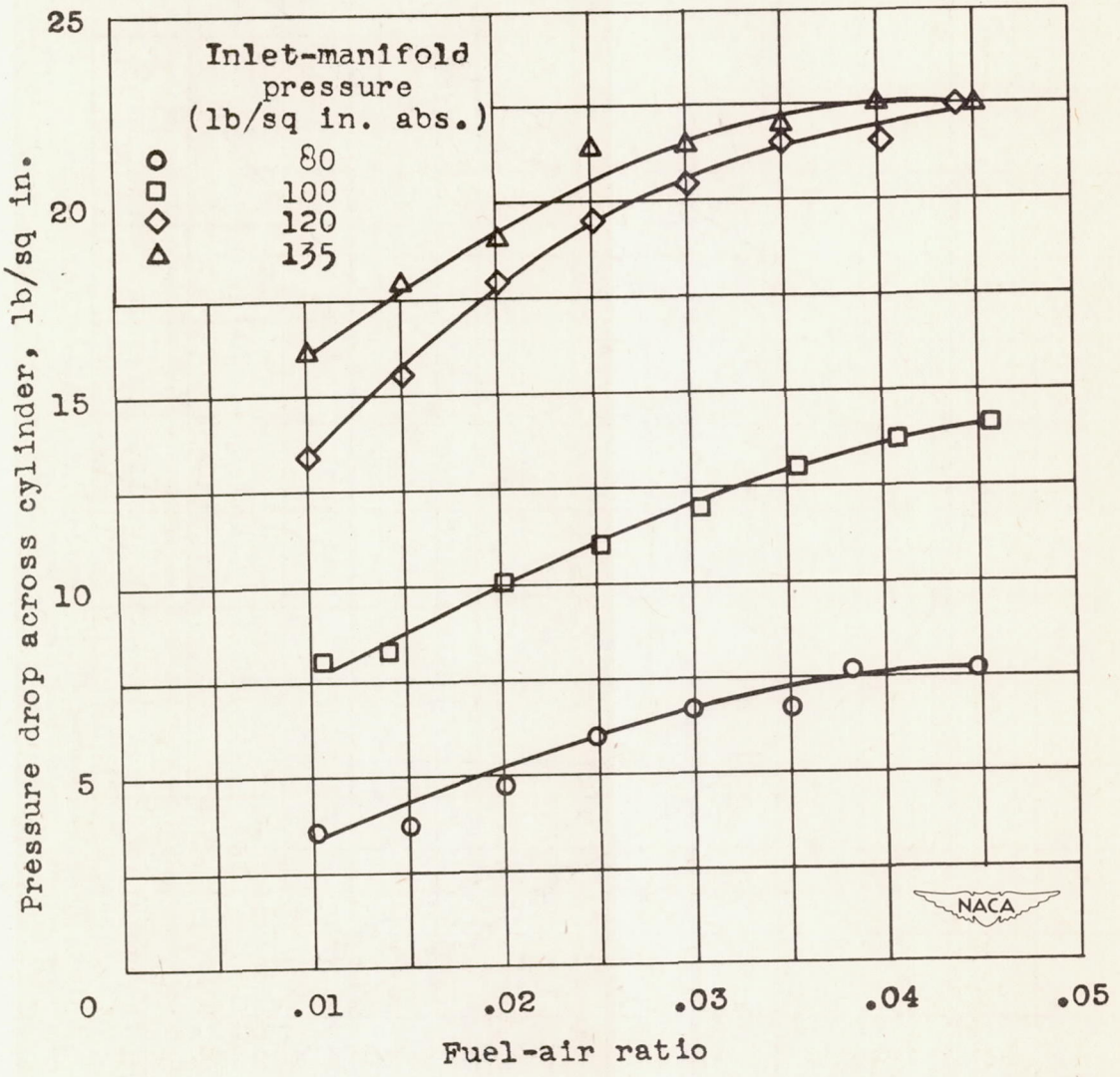


Figure 8. - Effect of inlet-manifold pressure and fuel-air ratio on cylinder pressure drop. Compression ratio, 5.25; inlet-manifold temperature, 400° F.

1077

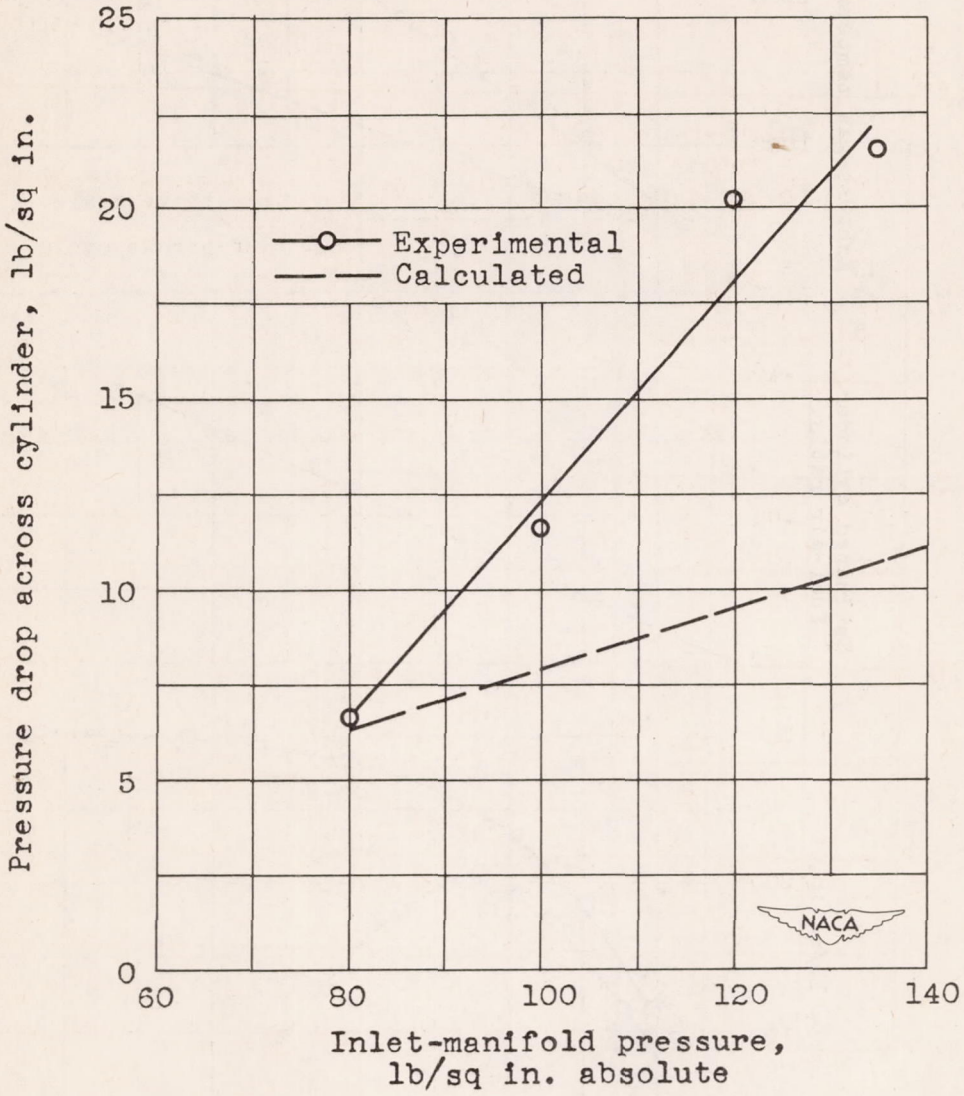


Figure 9. - Comparison of experimental and calculated values of cylinder pressure drop. Compression ratio, 5.25; inlet-manifold temperature, 400° F; fuel-air ratio, 0.03. Theoretical values are based on equation (2).

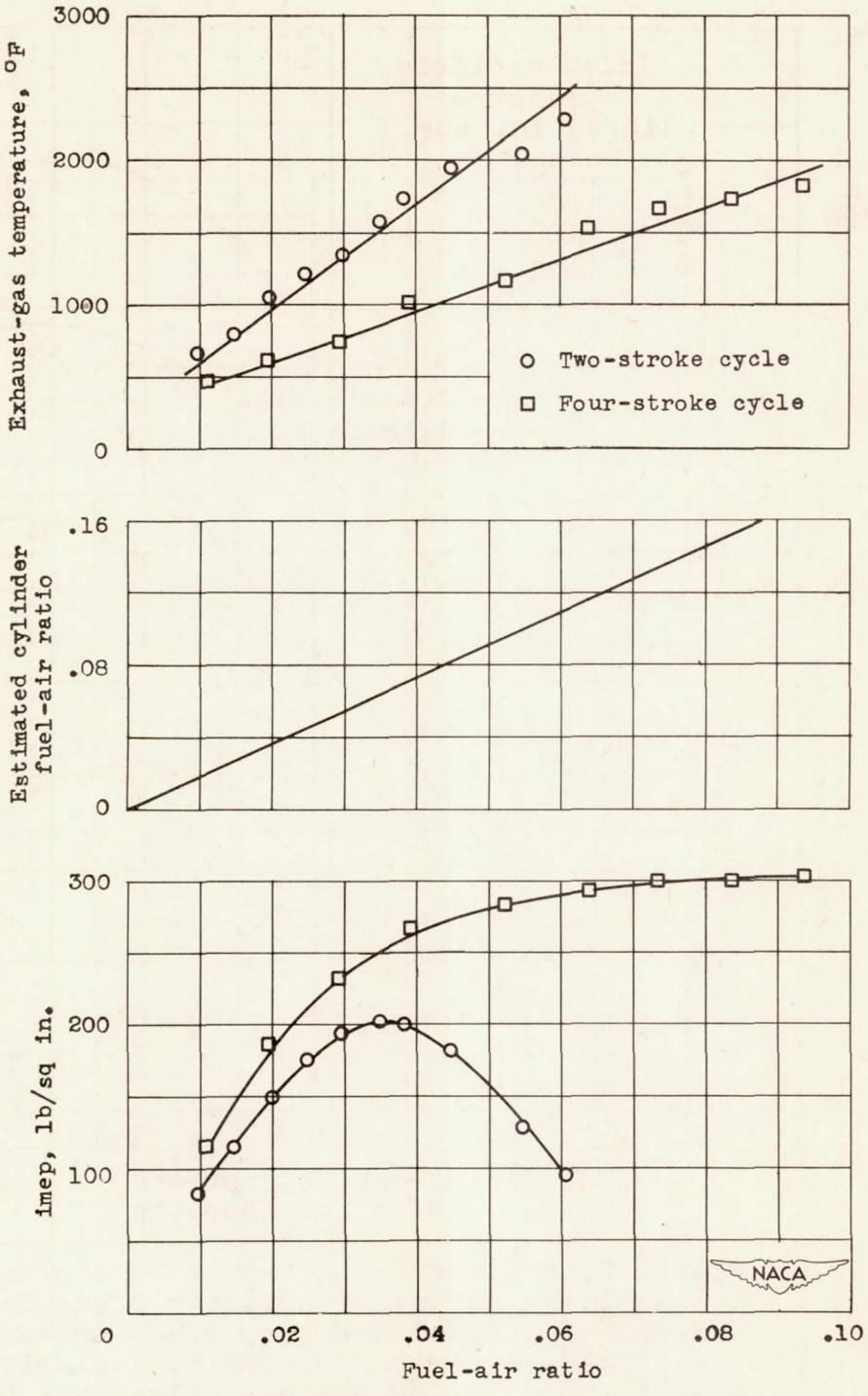


Figure 10. - Effect of over-all fuel-air ratio on performance of experimental cylinder with two-stroke and four-stroke cycle operation. Inlet-manifold temperature, 400° F; two-stroke cycle; compression ratio, 5.25; inlet-manifold pressure, 80 pounds per square inch absolute; four-stroke cycle; compression ratio, 4.6; inlet-manifold pressure, 100 pounds per square inch absolute.

1077

1077

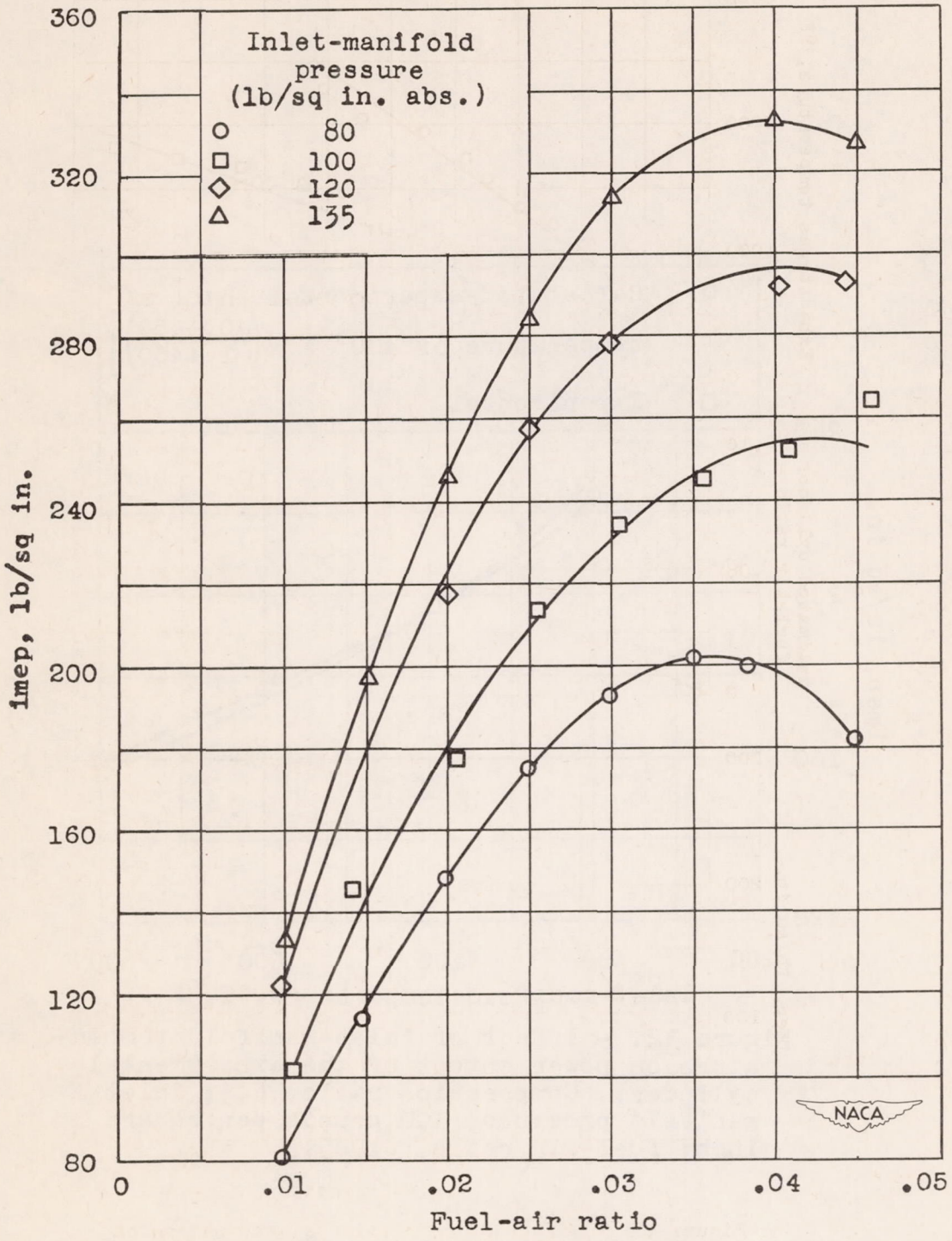


Figure 11. - Effect of inlet-manifold pressure and fuel-air ratio on power output of experimental cylinder. Compression ratio, 5.25; inlet-manifold temperature, 400° F.

1077

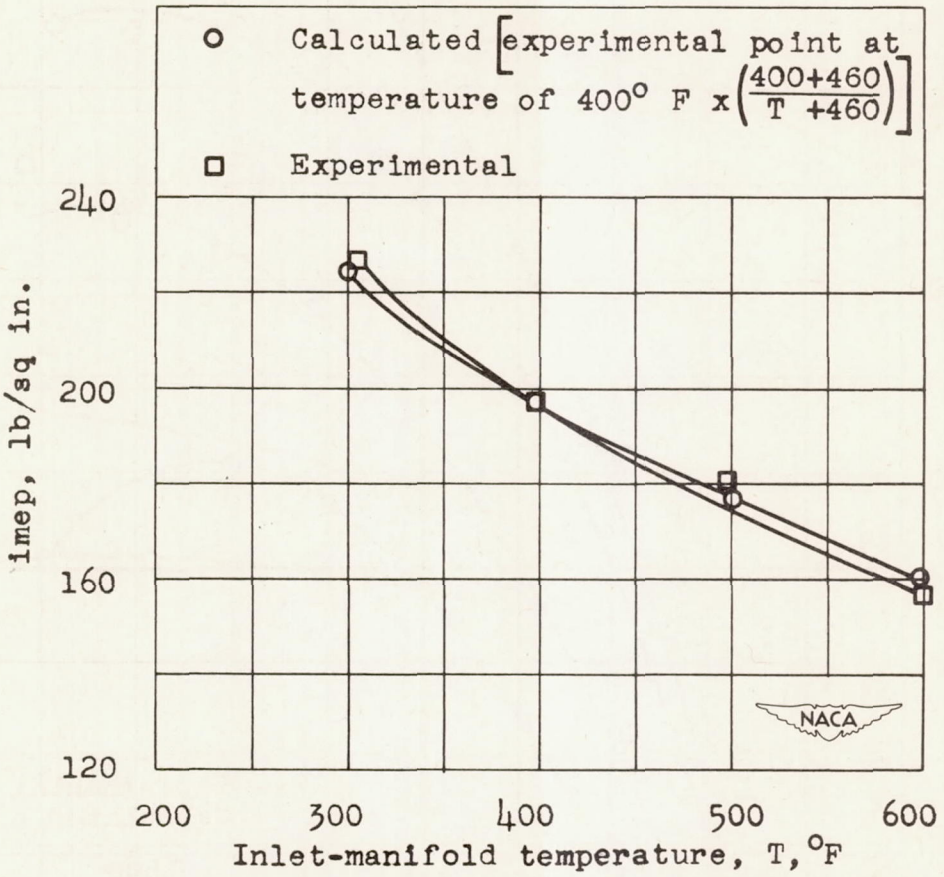


Figure 12. - Effect of inlet-manifold temperature on power output of the experimental cylinder. Compression ratio, 4.5; inlet-manifold pressure, 100 pounds per square inch; fuel-air ratio, 0.025.

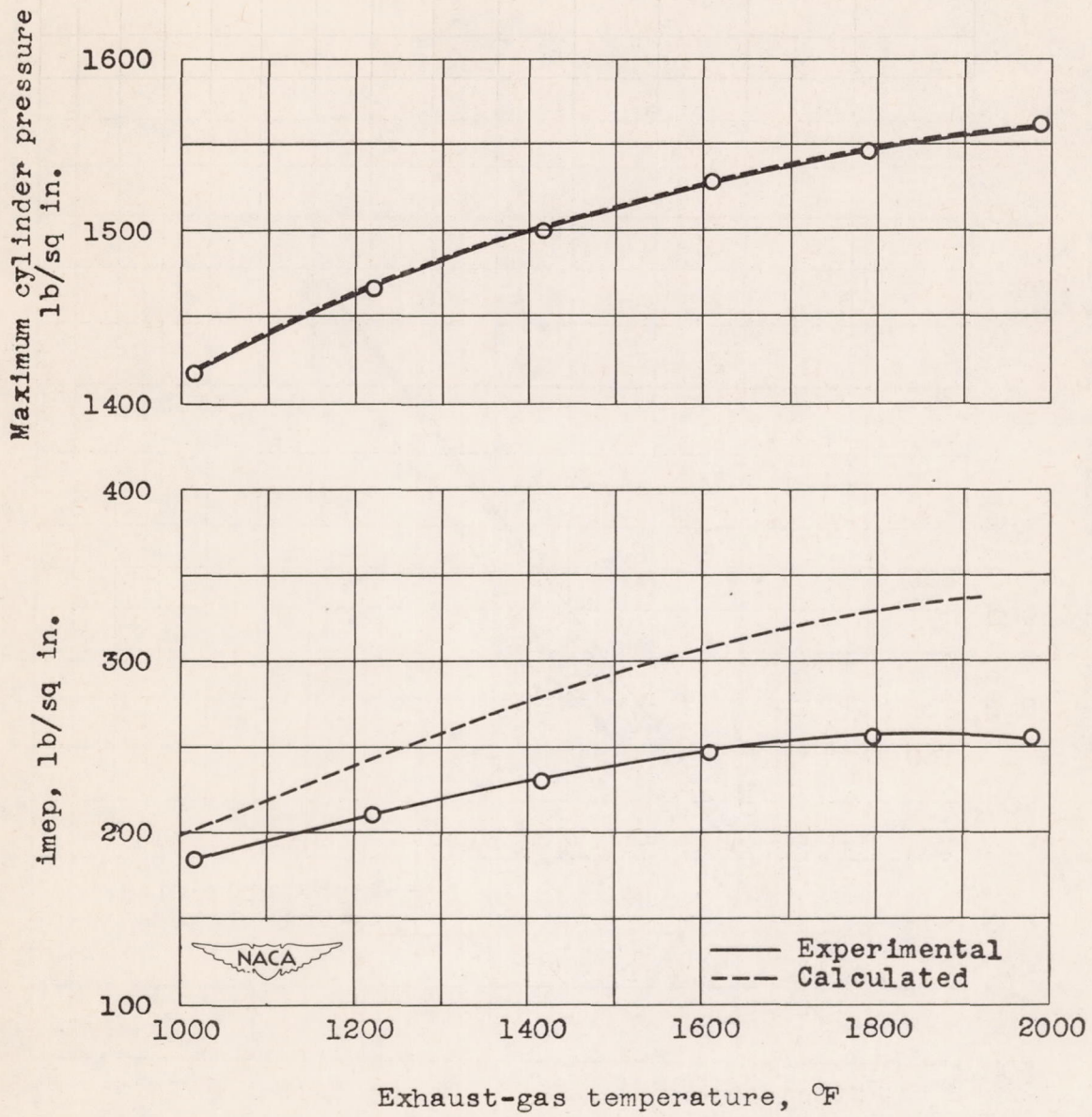


Figure 13. - Correlation of experimental and calculated values of indicated mean effective pressure for experimental cylinder. Inlet-manifold temperature, 400° F; inlet-manifold pressure, 100 pounds per square inch absolute.

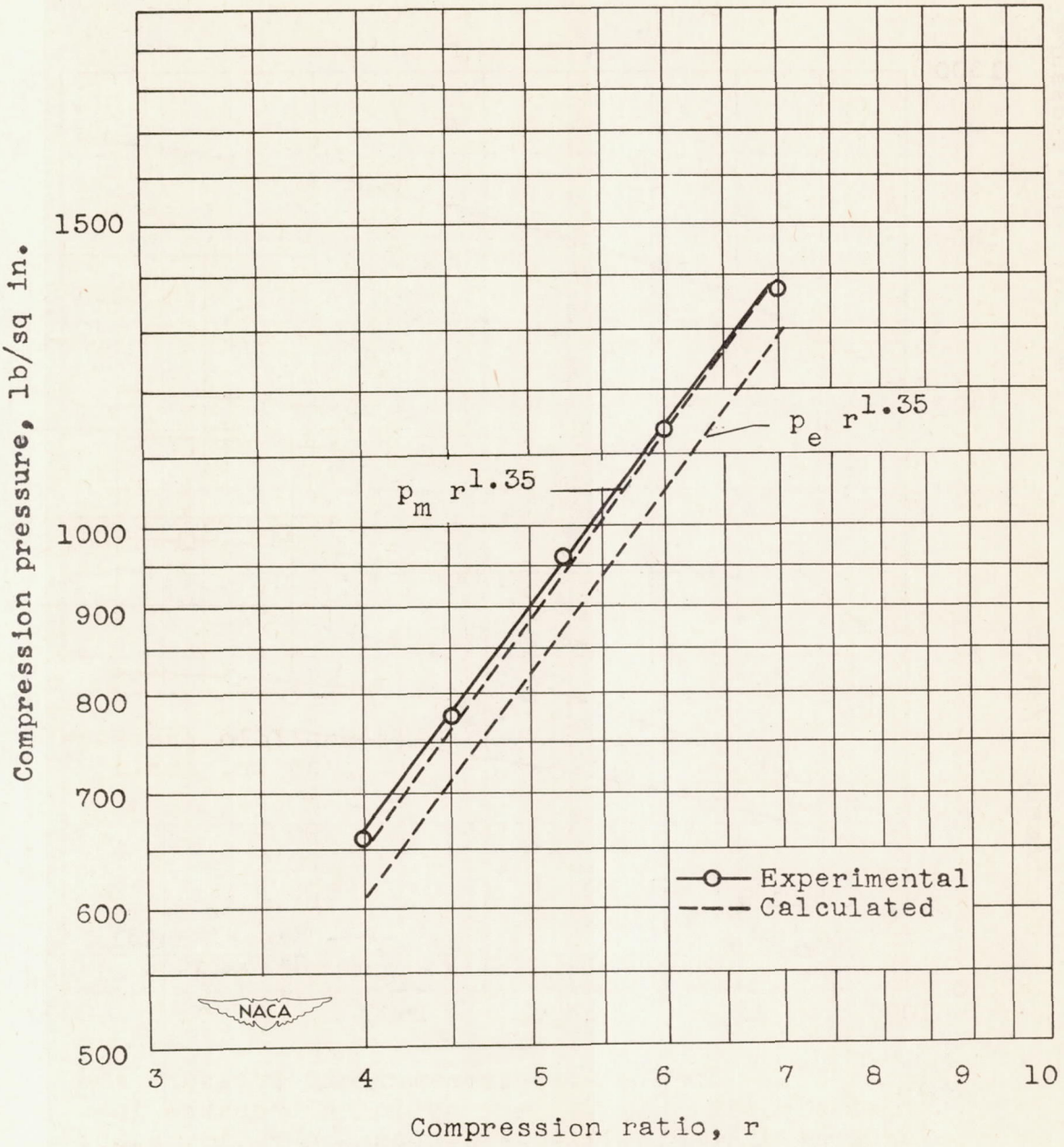


Figure 14. - Comparison of experimental and calculated values of compression pressures. Inlet-manifold temperature, 400° F; inlet-manifold pressure p_m, 100 pounds per square inch absolute; exhaust-manifold pressure p_e, 92.5 pounds per square inch absolute; exponent for compression, 1.35.

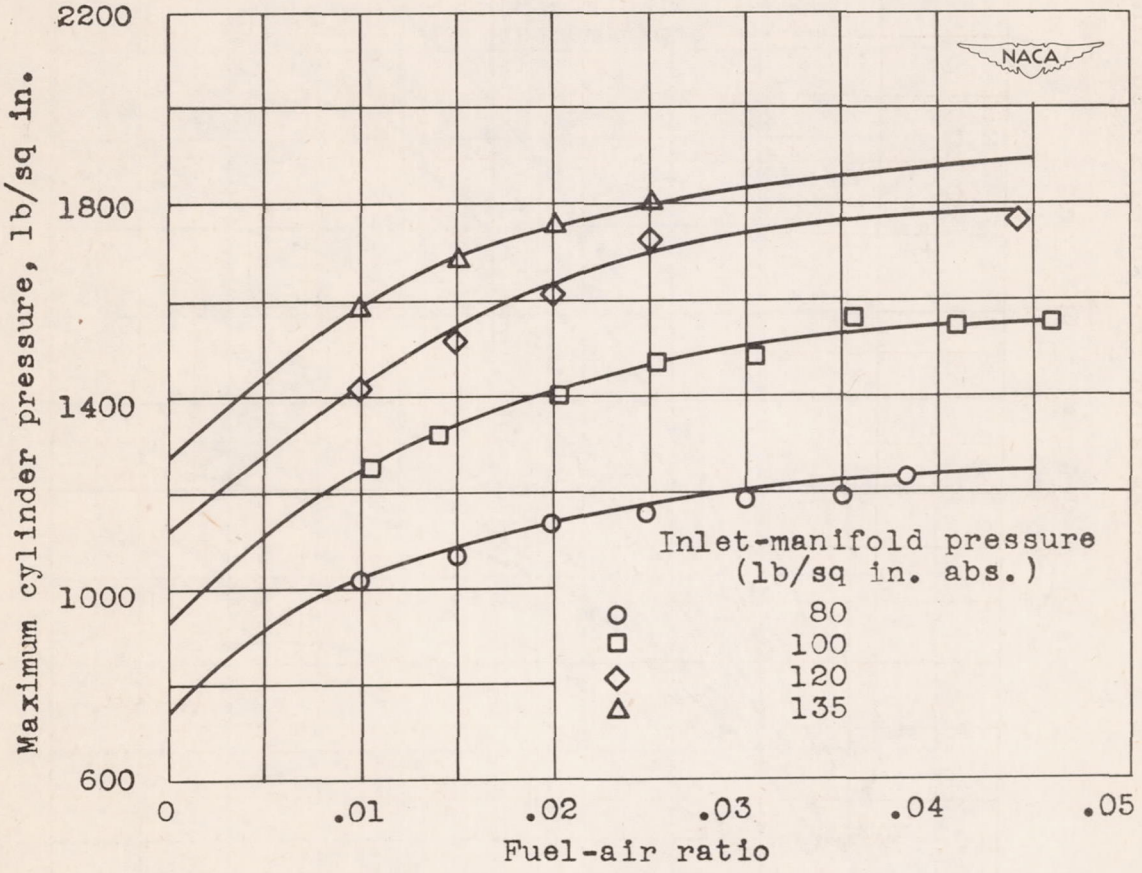


Figure 15. - Effect of inlet-manifold pressure and fuel-air ratio on maximum cylinder pressure in experimental cylinder. Compression ratio, 5.25; inlet-manifold temperature, 400° F.

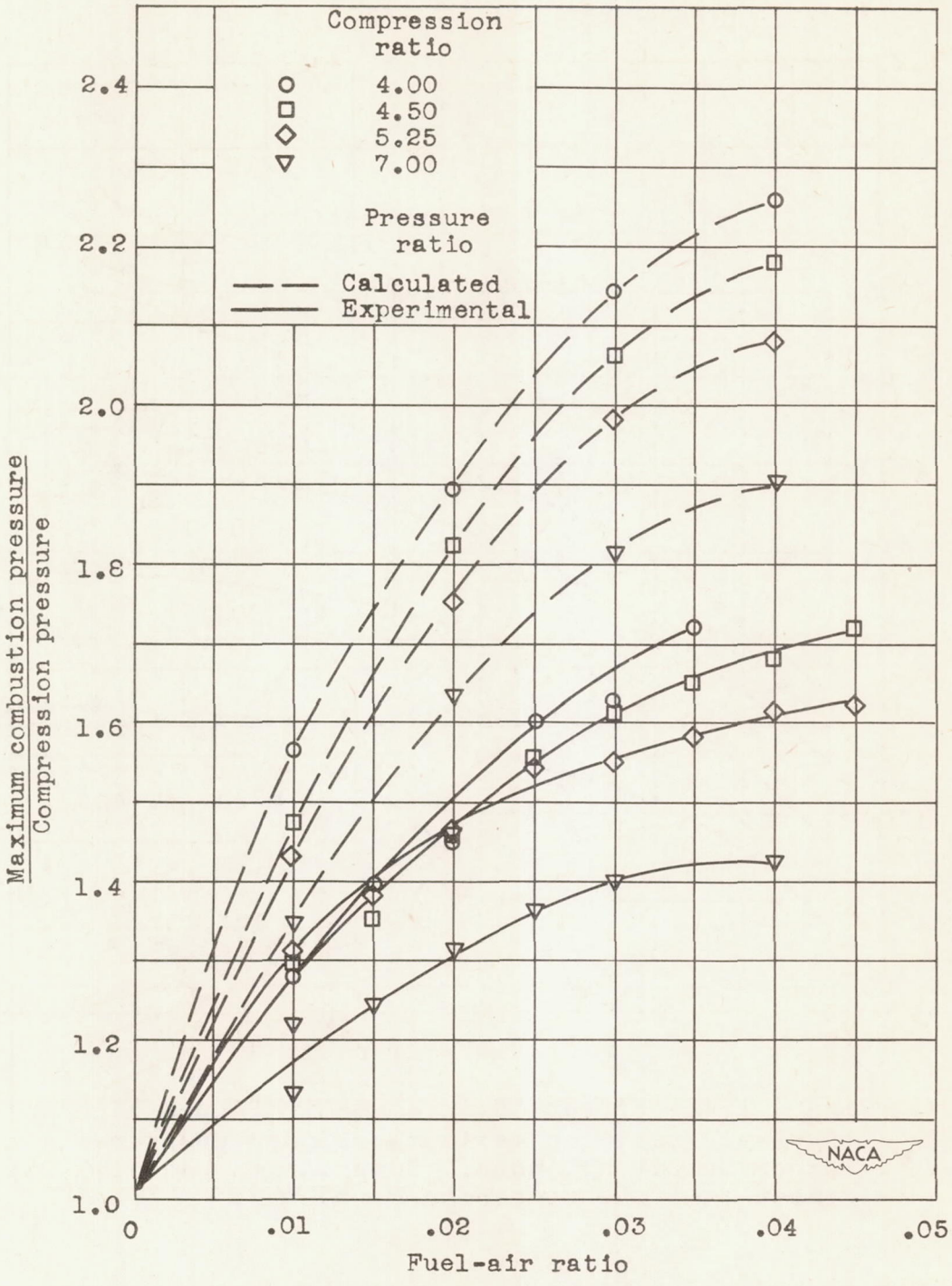


Figure 16. - Effect of compression ratio and fuel-air ratio on ratio of maximum combustion pressure to compression pressure. Inlet-manifold temperature, 400° F; inlet-manifold pressure, 100 pounds per square inch absolute.

1077

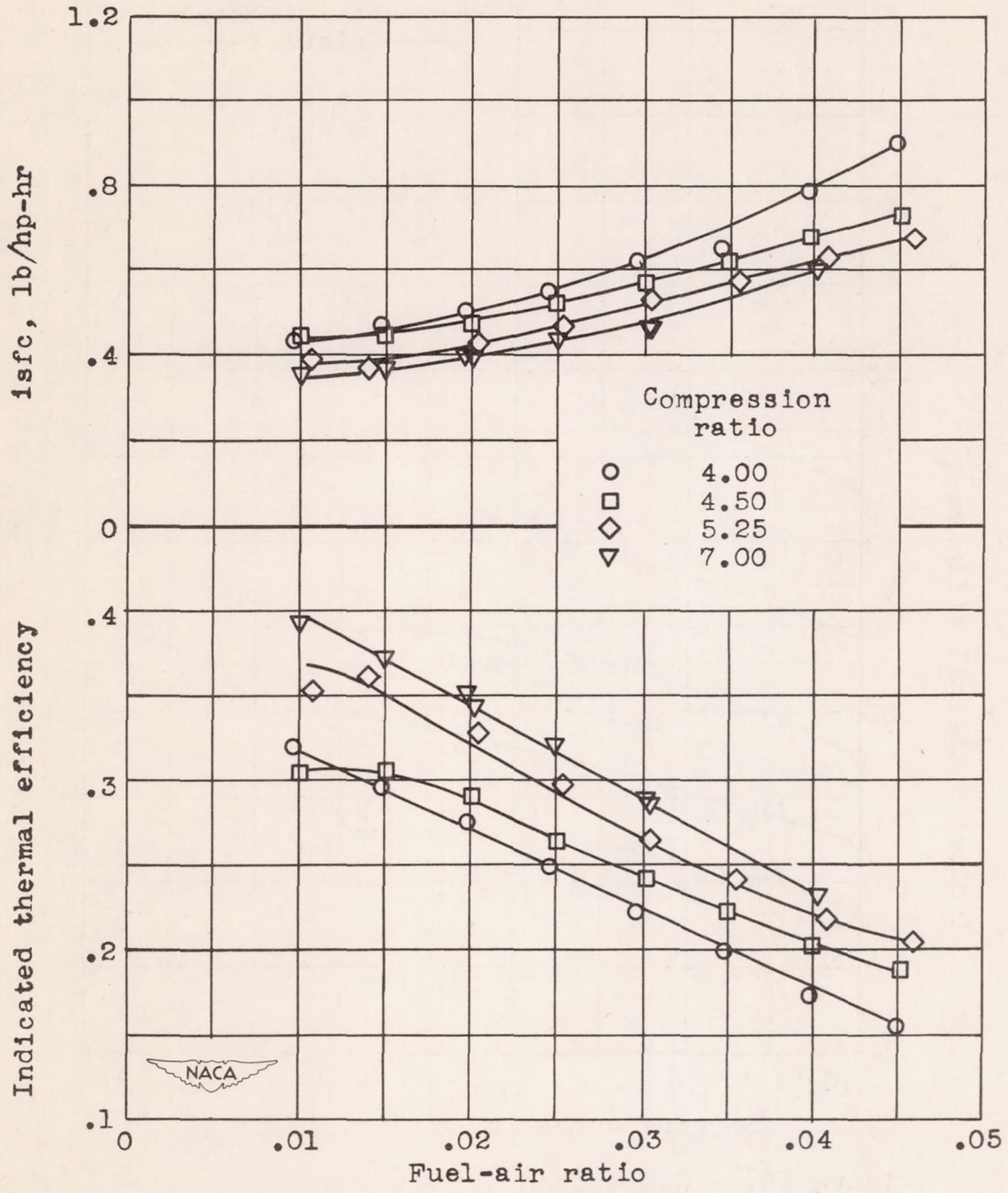


Figure 17. - Effect of fuel-air ratio and compression ratio on indicated efficiency of experimental cylinder. Inlet-manifold temperature, 400° F; inlet-manifold pressure, 100 pounds per square inch absolute.

1077

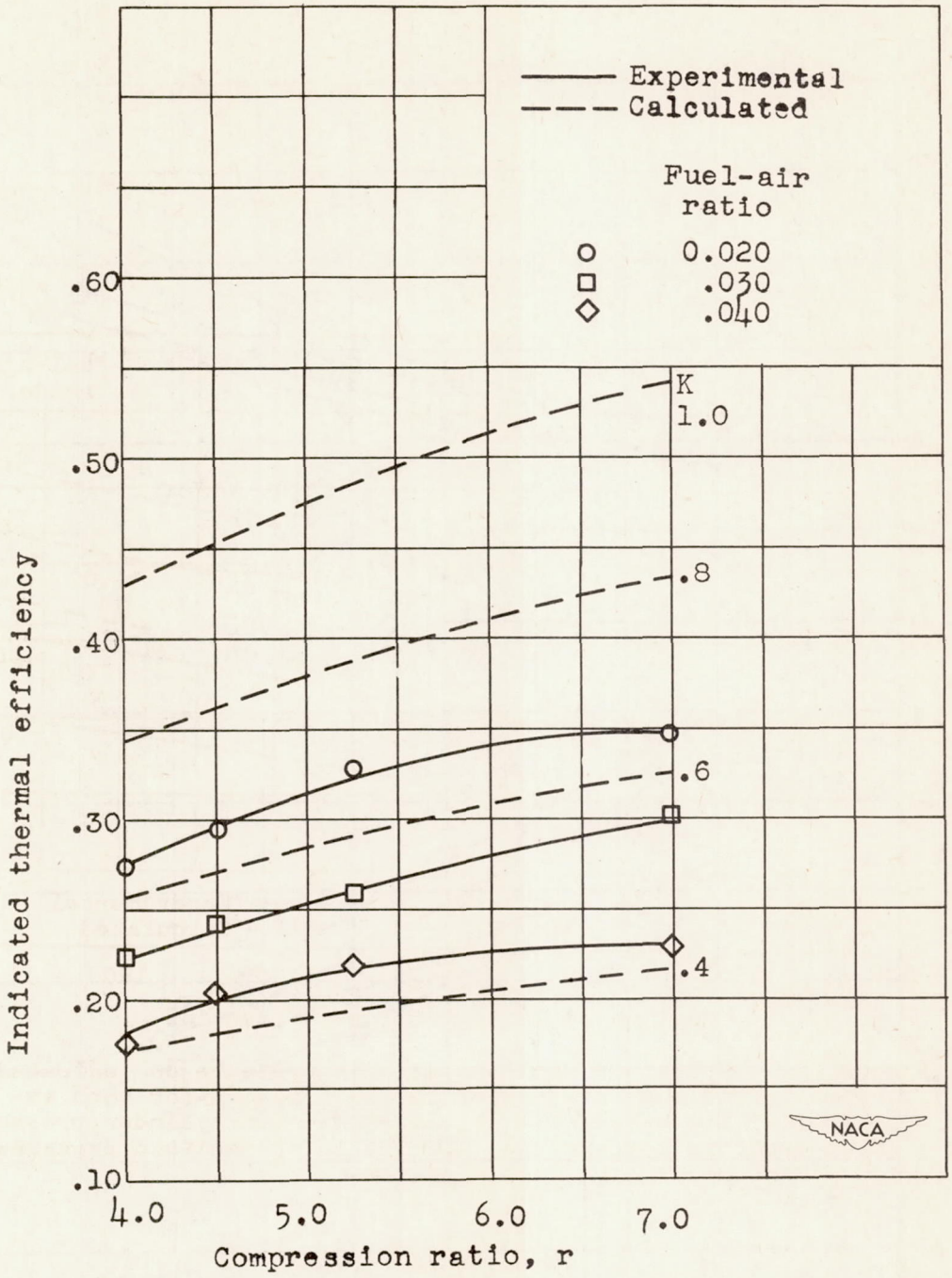


Figure 18. - Comparison of experimental and calculated indicated thermal efficiencies on basis of compression ratio. Inlet-manifold temperature, 400° F; inlet-manifold pressure, 100 pounds per square inch absolute; calculated thermal efficiency $\eta_t = K\left(1-\frac{1}{r^{0.4}}\right)$.

1077

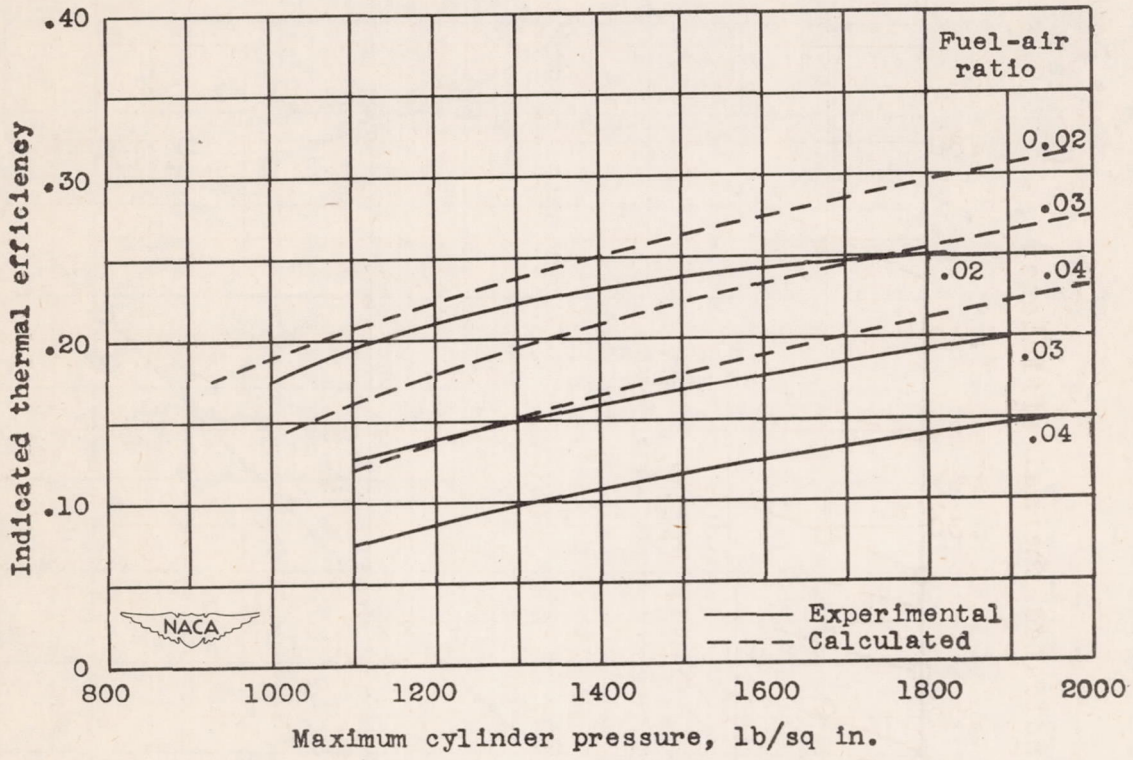


Figure 19. - Effect of maximum cylinder pressure on indicated thermal efficiency at several fuel-air ratios for both experimental and calculated values of maximum cylinder pressure. Inlet-manifold temperature, 400° F; inlet-manifold pressure, 100 pounds per square inch absolute.

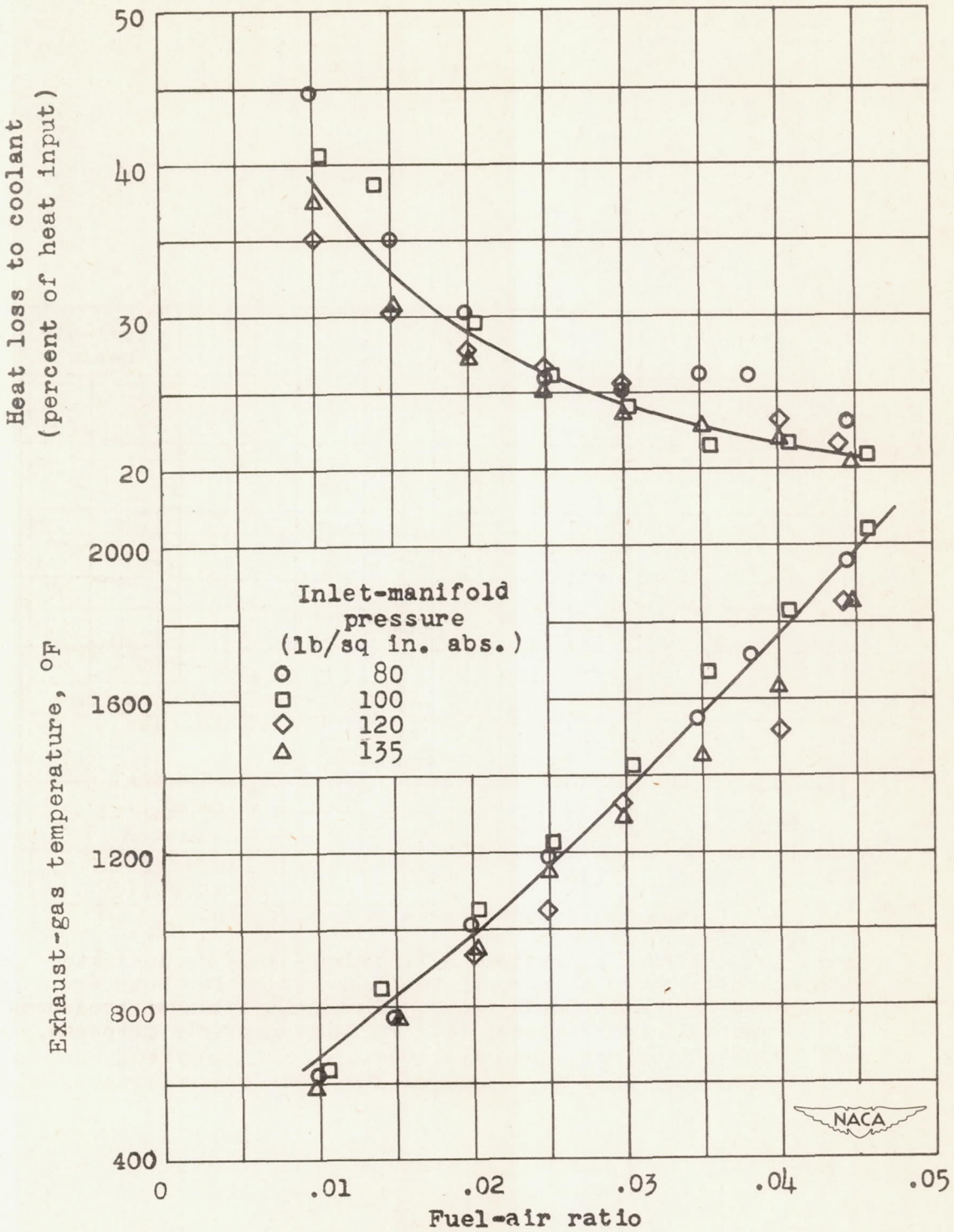


Figure 20. - Variation of heat loss and exhaust-gas temperature of experimental cylinder with fuel-air ratio. Compression ratio, 5.25; inlet-manifold temperature, 400° F.

1077

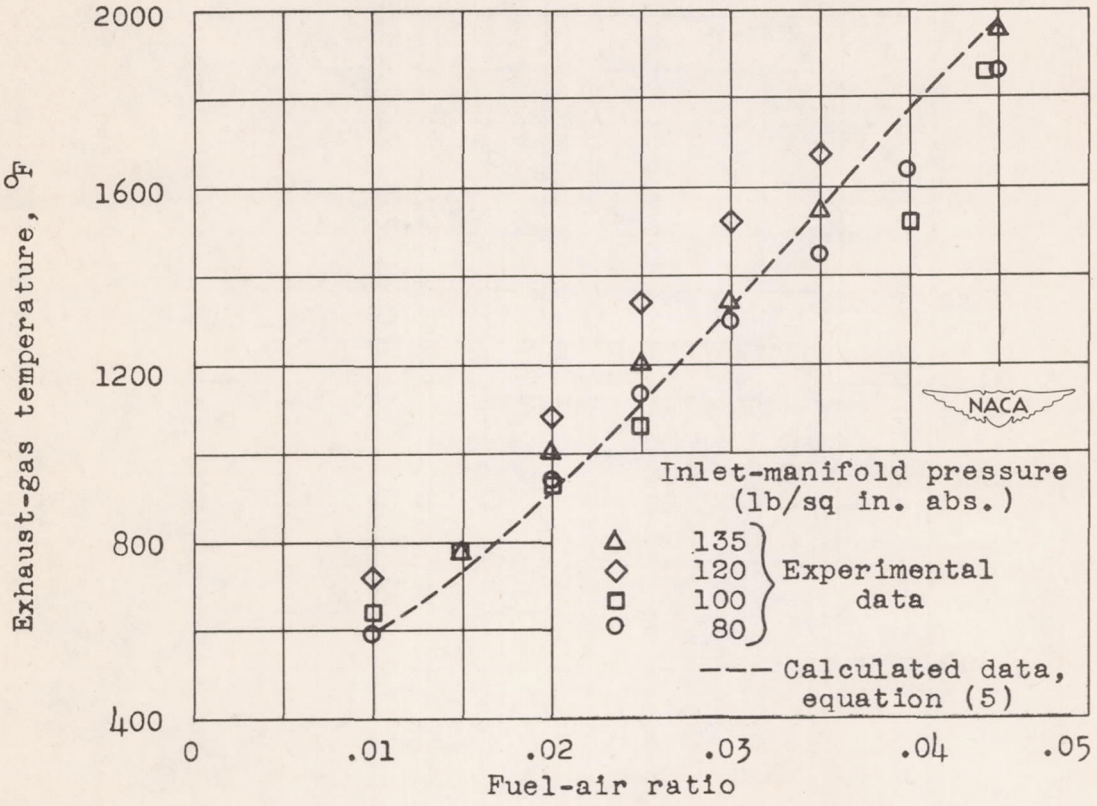


Figure 21. - Comparison of experimental and calculated exhaust-gas temperatures. Inlet-manifold temperature, 400° F; compression ratio, 5.25. Calculation made at inlet-manifold pressure of 100 pounds per square inch.

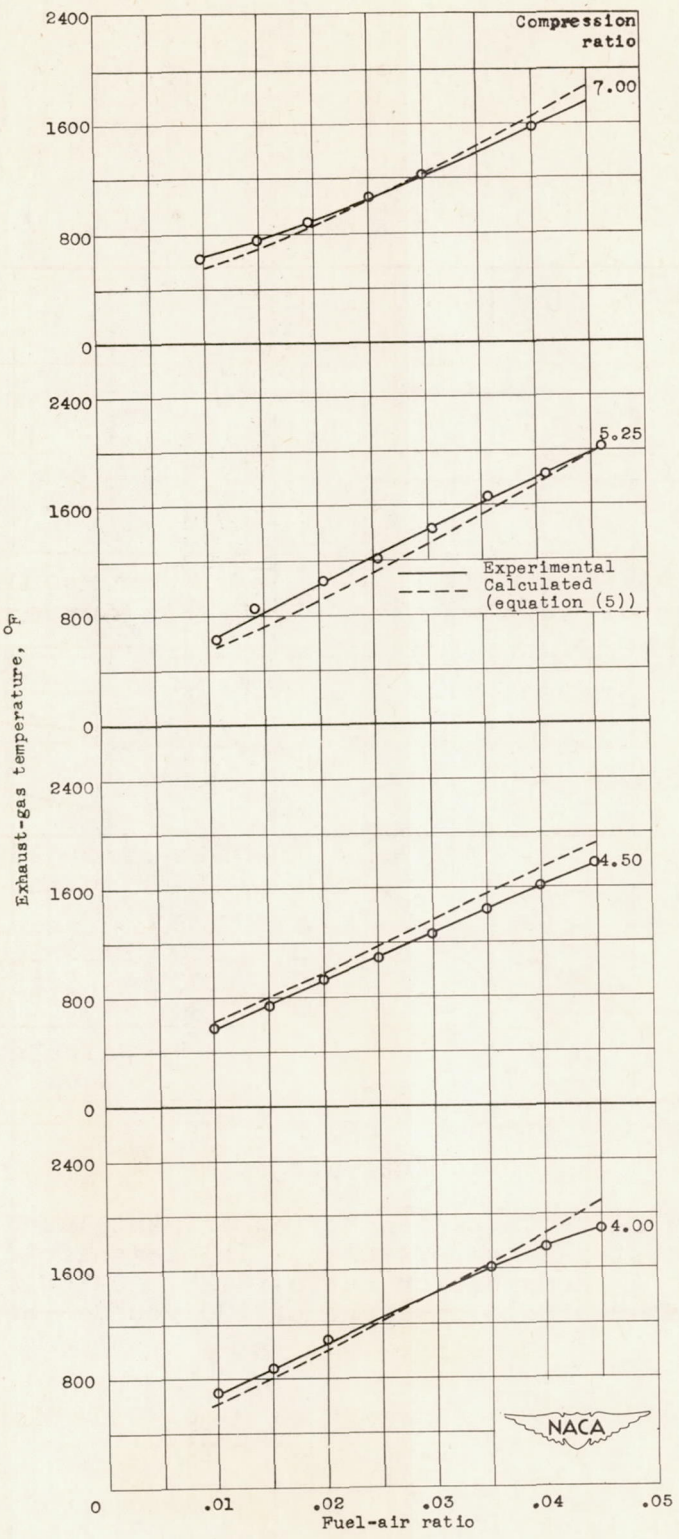


Figure 22. - Comparison of experimental and calculated values of exhaust-gas temperature at various compression ratios and fuel-air ratios. Inlet-manifold temperature, 400° F; inlet-manifold pressure, 100 pounds per square inch absolute.

1077

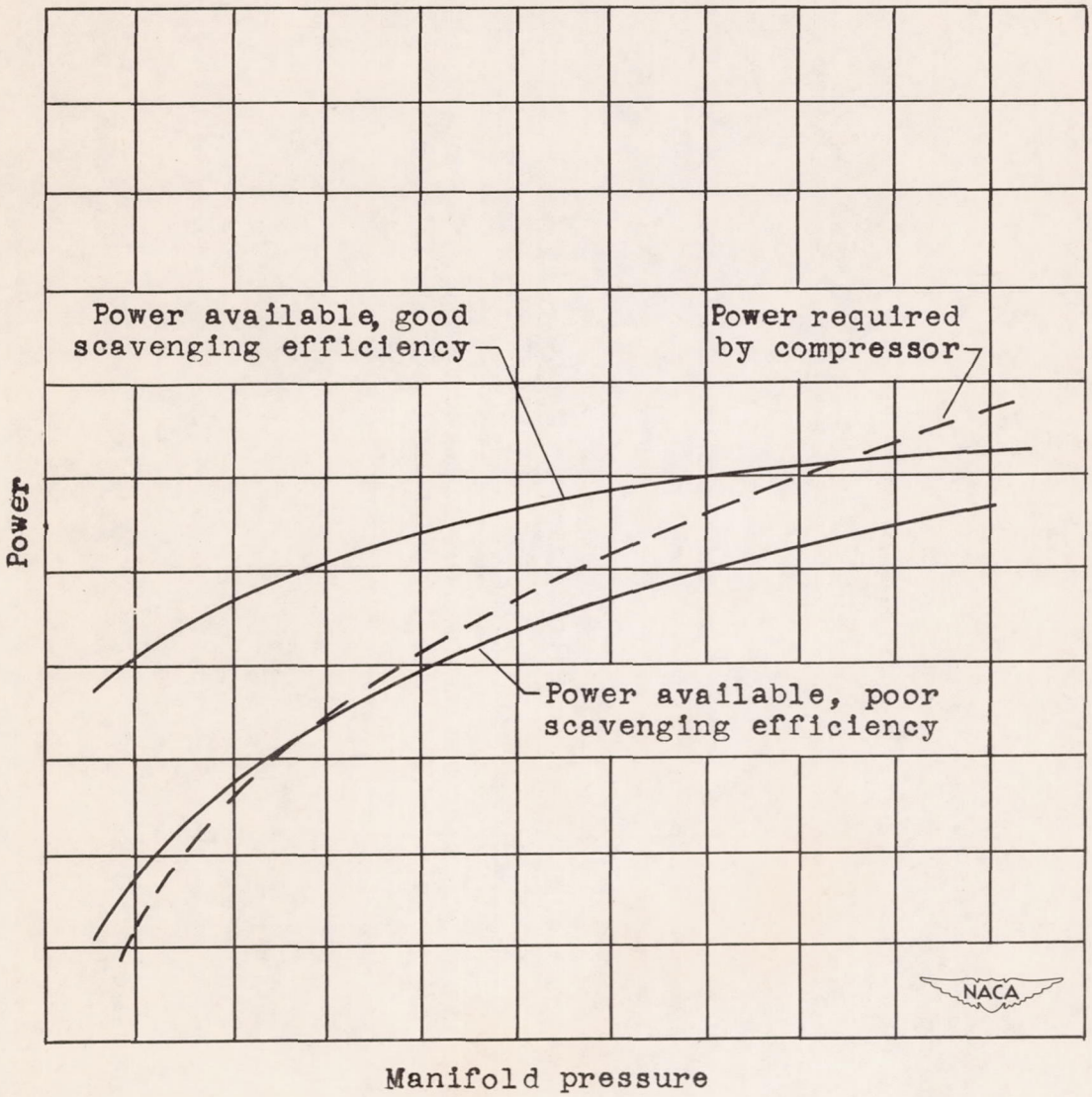


Figure 23. - Compressor and engine power relations in gas-generator engine.